Bollettino di Geofisica Teorica ed Applicata Vol. 55, n. 3, pp. 589-616; September 2014
DOI 10.4430/bgta0122

Multidisciplinary analyses to understand the tectonic activity and the evolution of the North Anatolian Fault in the Hersek Peninsula (İzmit Gulf, Turkey)

E. Forte[1], M. Sugan[2], A. Del Ben[1], M. Pipan[1], L. Gasperini[3] and H. Kurt[4]

[1] *Dep. of Mathematics and Geosciences, University of Trieste, Italy*
[2] *OGS National Institute of Oceanography and Experimental Geophysics, Udine, Italy*
[3] *ISMAR (Institute of Marine Sciences), National Research Council, Bologna, Italy*
[4] *Dep. of Geophysical Engineering, Istanbul Technical University, Turkey*

(Received: December 11, 2013; accepted: March 7, 2014)

ABSTRACT Despite several offshore data are available, a general model of the central part of the İzmit Gulf is still a challenge and only few measurements have been done on the Hersek peninsula. This area is a key point not only because represents the only onshore segment of the North Anatolian Fault (NAF) within the central part of the İzmit Gulf, but also because the new Istanbul-İzmit highway will cross such gulf in this zone, with a suspension bridge, which will be the second longest bridge of such type in the world. This paper, integrating different analyses and data sets aims verifying at some of the present hypotheses. In particular, we propose the joint interpretation of new seismic reflection profiles from the Hersek Peninsula, as well as geophysical, remote sensing and geological data from the İzmit Gulf (Sea of Marmara, Turkey), close to the epicenter of the 1999, M_w 7.4 İzmit earthquake, to identify shallow-crustal deformations associated with the NAF. Our seismic reflection profiles, which are the first onshore two-components records within the İzmit Gulf, image compressive features that form a structural high cut by the principal deformation zone of the NAF. The observed transpressive stress pattern appears to be the main factor contributing to the physiography of the peninsula, together with the growth northwards of the Yalakdere River deposits. We demonstrate that this pattern is compatible with an 8° bending of the NAF strand. Based on these new data, we propose a kinematic model for the evolution of this structure around the Hersek Peninsula during Holocene, and we test our reconstruction using a finite-elements numerical simulation model of the stress/strain distribution.

Key words: North Anatolian Fault, Hersek Peninsula, İzmit Gulf, continental strike-slip fault, reflection seismic, finite-elements structural modelling.

1. Introduction

The study of the İzmit Gulf is crucial to understand the kinematics of the North Anatolian Fault (NAF) in the Marmara Sea region, and to assess seismic risk and future earthquake scenarios through enhanced knowledge of space and time distribution of the tectonic stress.

The Marmara Sea (Fig. 1) is a pull-apart system created at the transition between the pure strike-slip tectonic regime of the eastern part of the NAF and the extensional system of the Aegean Sea to the west (e.g., Barka and Kadinsky-Cade, 1988). The transition between different stress conditions is responsible for the formation of several basins where strike-slip and extension interfere [a comprehensive review of the NAF can be found, for instance, in Şengör (1979), Bozkurt (2001), and Şengör *et al*. (2004)].

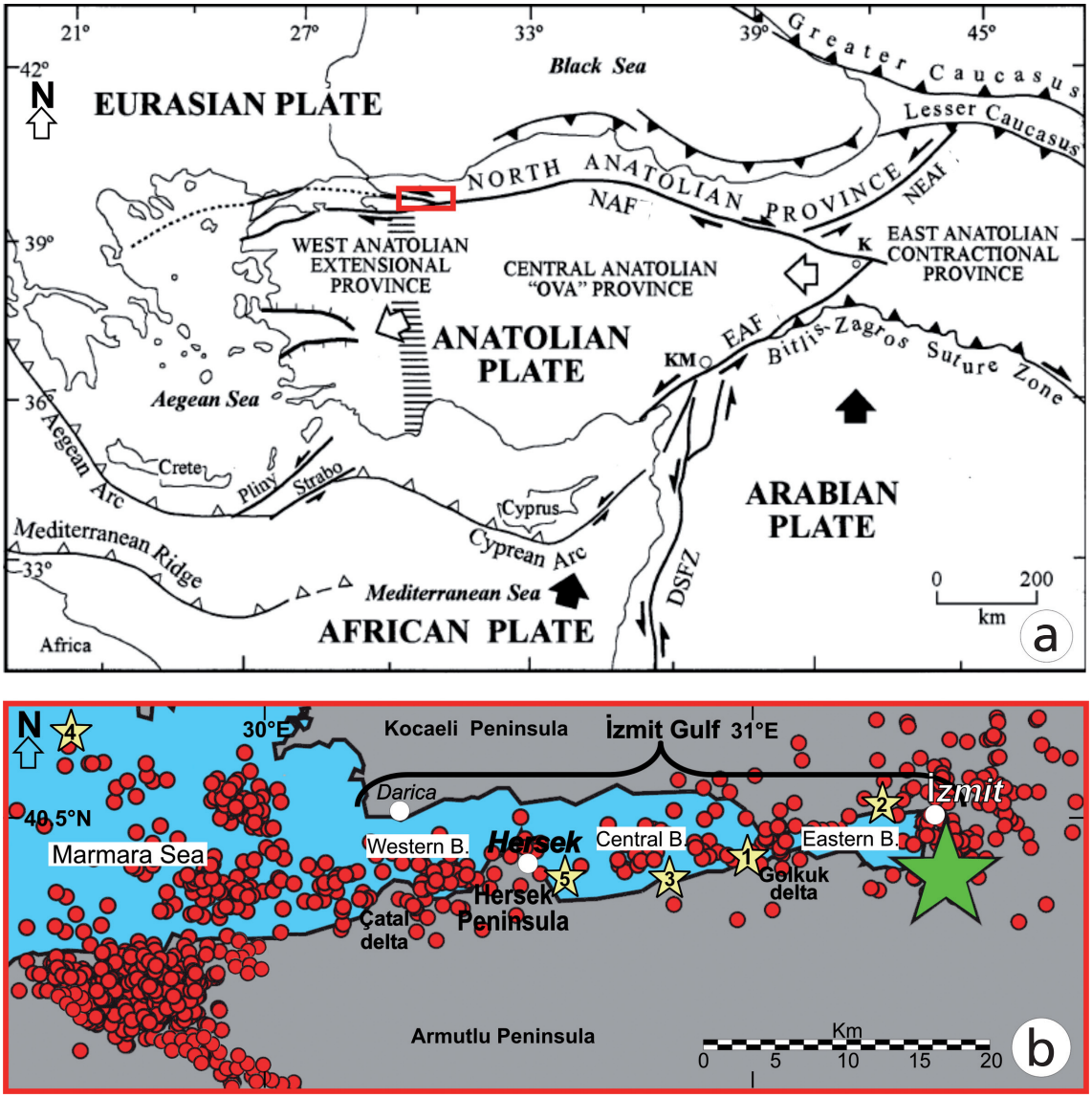

Fig. 1 - a) Simplified tectonic scheme of the eastern Mediterranean Sea and the Middle East with the location of the North Anatolian Fault (NAF), the East Anatolian Fault (EAF) and the North-East Anatolian Fault (NEAF). The red rectangle represents the İzmit Gulf zone mapped in (b). b) Location of the main shock (17 August 1999, green star), of the aftershocks in the 17 August - 24 September 1999 interval (red dots) and of the historical main seismic events (yellow stars), [from Şengör *et al*. (1985) and Polat *et al*. (2002), modified]. The historical seismicity is from Ambraseys (2002b): 1) 478, 7.3 M_s; 2) 554, 6.9 M_s; 3) 1719, 7.4 M_s; 4) 1754, 6.8 M_s; 5) 1894, 7.3 M_s.

Geophysical surveys of the Marmara Sea provided enhanced models of structure and evolution after the İzmit, 7.4 M_w (referred in literature also as Kocaeli or Gölcük) and Düzce 7.2 M_w earthquakes (August 17 and November 12, 1999, respectively). These data suggest that the Marmara basins formed during an initial extensional phase and became less active or inactive after the development of a new segment of the NAF (Fig. 1a), at large scale E-W oriented, crossing all the basins (Gökaşan *et al*., 2001, 2003; İmren *et al*., 2001; Le Pichon *et al*., 2001; Alpar and Yaltırak, 2002; Kuşçu *et al*., 2002; Polonia *et al*., 2004; Şengör *et al*., 2004; Dolu *et al*., 2007). Such new segment was labeled as "New Marmara Fault" [NMF: Gökaşan *et al*. (2003)], "Main Marmara Fault" (İmren *et al*., 2001), or "Great Marmara Fault" [GMF: Le Pichon *et al*. (1999), Alpar and Yaltırak (2002), Yaltırak (2002)] referring to the whole Marmara Sea or, more specifically, just to the İzmit Gulf.

Deep seismic exploration was extensively conducted in the Marmara Sea, and in particular in the Çinarcik basin (Parke *et al*., 1999; Okay *et al*., 2000; Rangin and Le Pichon, 2004; Carton *et al*., 2007, Kurt *et al*., 2013), while Demirbağ *et al*. (2003) used deep-towed high-resolution seismic profiling; but only relative shallow seismic data are available to date in literature for the İzmit Gulf (Gökaşan *et al*., 2001; Alpar and Yaltırak, 2002; Kuşçu *et al*., 2002; Çağatay *et al*., 2003; Polonia *et al*., 2004; Cormier *et al*., 2006), except the ones published by Kurt and Yücesoy, 2009 (1.5 s TWT).

The study and the location of the tectonic structures in the İzmit Gulf is based on different geophysical data sets (high-resolution and deep seismics, multibeam sonar, side scan sonar) calibrated by sea bottom core samples and by borehole data (Gökaşan *et al*. 2001; Alpar and Yaltırak 2002; Çağatay *et al*., 2003; Polonia *et al*., 2004; Cormier *et al*., 2006; Kurt and Yücesoy, 2009; Gasperini *et al*., 2011). Moreover, evolutional model of this area considered also the vertical displacement, occurring in combination with the principal strike-slip movement and correlated with different structural models (Alpar and Yaltırak, 2002, 2003; Emre and Awata, 2003; Polonia *et al*., 2004; Cormier *et al*., 2006; Dolu *et al*., 2007).

Despite these studies, the location of active NAF segments in the western and central basins of the İzmit Gulf is still matter of debate. Some authors place the NAF along the southern border of the central basin or, alternatively, across the Hersek Peninsula (see e.g., Alpar and Yaltırak, 2002), while others suggest that the NAF consists of several segments. The distribution of epicenters of the major earthquakes along the NAF shows a migration from east to west that indicates a progressive concentration of the stress at the western termination of the fault followed by catastrophic releases (Özalaybey *et al*., 2002). The location of the western termination of the rupture associated to the August 17, 1999 earthquake is another matter of debate. Different geophysical offshore data obtained in the İzmit Gulf, however, allowed to defining the neotectonic elements at various scales, together with estimating the slip rate during the last 40 kyrs (Gökaşan *et al*., 2001; Kuşçu *et al*., 2002; Alpar and Yaltırak, 2002, 2003; Çağatay *et al*., 2003; Gökaşan *et al*., 2003; Polonia *et al*., 2004; Cormier *et al*., 2006; Dolu *et al*., 2007; Gasperini *et al*., 2011). Moreover, seismological studies focused on both aftershocks (Polat *et al*., 2002) and slip/stess distribution (Bouchon *et al*., 2002; Aochi and Madariaga, 2003), show clear co- and post-seismic effects far to the west from the Hersek Peninsula. Nevertheless, the correlation and integration of such data failed to provide a single coherent model.

Measurements of slip (GPS, vertical/horizontal slip components) and paleoseismic studies within trenches, performed onshore to quantify the displacements related to the 1999 events

(Lettis *et al.*, 2000, 2002; Witter *et al.*, 2000; Barka *et al.*, 2002; Gülen *et al.*, 2002; Awata *et al.*, 2003; Emre and Awata, 2003; Kozaci *et al.*, 2011) do not clarify: whether and where the NAF crosses the Hersek Peninsula, which is the fault geometry and whether it was activated during the 1999 earthquakes. In fact the conclusions obtained in the most recent publications about this area are not coherent and often contrasting (Özaksoy *et al.*, 2010; Kozaci *et al.*, 2011; Uçarkuş *et al.*, 2011), even if clear 1999 earthquake surface ruptures have been observed by integrated high-resolution multibeam, side-scan sonar and Remotely Operated Vehicle (ROV) data far west from the Hersek Peninsula (Gasperini *et al.*, 2011).

Hersek Peninsula has been a very important and strategic location since the Roman period because it is close to the northern shore and to the route to Nicea (at present İznik). Additionally, this area became more and more significant during the Constantine Empire (272-337 A.D.). His mother, St. Helen, was born in the village nowadays called Hersek and previously called Helenopolis in her honor. At present there are nearly no remains of public and private buildings and infrastructures of various ages, due to the battles fought in the area and the strong earthquakes that occurred (Ambraseys, 2002a, 2002b).

This paper focuses on the tectonic study of the Hersek Peninsula (Fig. 1b), which represents a pivotal element in the definition of the tectonic and structural model of the whole İzmit Gulf. We performed onshore geological surveys and acquired P-waves and S-waves seismic reflection profiles to understand the origin and the evolution of the peninsula. The new seismic images were interpreted in the frame of up to date geomorphological and stratigraphic data from the area. Further correlation was established with the offshore data extensively collected in the İzmit Gulf after the 1999 events (Alpar, 1999; Gökaşan *et al.*, 2001, 2003; Kuşçu *et al.*, 2002; Alpar and Yaltırak, 2002; Çağatay *et al.*, 2003; Polonia *et al.* 2004; Cormier *et al.*, 2006; Dolu *et al.*, 2007; Okyar *et al.*, 2008; Kurt and Yücesoy, 2009) and with the onshore data available both from literature and collected for this research (see also Forte *et al.*, 2009).

Our tectono-kinematic model for the recent (Holocenic) evolution of the Hersek Peninsula was tested using a numerical simulation of stress and strain distribution with scaled dimensions.

2. Geological and geomorphological setting

2.1. Physiography of the İzmit Gulf and morphology of the Hersek Peninsula

The İzmit Gulf is an E-W elongated inlet of the eastern Marmara Sea between the Armutlu and the Kocaeli peninsulas to the south and north, respectively. Its total length is about 50 km and the width ranges between 2 and 10 km. The minimum width occurs to the north of the Hersek Peninsula, a triangularly shaped promontory that intrudes the İzmit Gulf by over 5 km (Fig. 1b).

The İzmit Gulf can be divided into three interconnected basins: the Western (or Darica) Basin is connected to the Marmara Sea by a deep canyon; the Central (or Karamürsel) Basin is the largest one, with a maximum depth of about 208 m (Kuşçu *et al.*, 2002; Okyar *et al.*, 2008); the Eastern (or İzmit) Basin exhibits maximum depth not exceeding 40 m (Gökaşan *et al.*, 2001; Kuşçu *et al.*, 2002; Alpar and Yaltırak, 2002, 2003; Çağatay *et al.*, 2003). Two relatively shallow sills, located to the north of the Hersek Peninsula (minimum depth 54 m) and of Gölcük

(minimum depth 33 m), separate the three basins. The coastal plain around the Gulf of İzmit is a few hundred metres wide, if we exclude the İzmit urban area (eastern sector), and the SW coast, with several fan-deltas.

Only minor streams enter presently the gulf from the north, while larger watercourses flow from the south. The Yalakdere and Kılıçdere rivers have respectively formed the Hersek and Çatal deltas. The Çatal delta has an areal extent of about 8 km^2, and protrudes by 2.5 km into the sea showing a maximum width of approximately 5 km. The Hersek delta is part of the most prominent peninsula of the İzmit Gulf, with an areal extent of more than 25 km^2.

From a geological and geomorphological point of view, the so-called Hersek delta (or Hersek Peninsula), with N-S and E-W dimensions of about 5 and 7 km, respectively, is a complex structure, comprised of three different zones: a fan-delta, a lagoon, and a northern area characterized by the presence of a topographic high called Dedeler Hill. Detailed analysis of digital maps (1:1000) and satellite data, in conjunction with our seismic reflection images, enabled a geological analysis of each unit forming the Hersek Peninsula.

1) Fan-delta

The Yalakdere River has south to north course, carving the Armutlu Peninsula relief and reaching with a narrow (about 250 m) gorge an alluvial plain (fan-delta) usually referred as Hersek Peninsula or Hersek delta. The total length of the river is approximately 35-40 km and there are several affluent streams. We analyzed the digital topographic data (1:1000) and obtained a detailed Digital Terrain Model (DTM) to evaluate the fan-delta morphology and determine the slope and the terrain aspect. Moreover, using satellite data we localized a complex paleo-river network and other morphological features (Figs. 2 and 3).

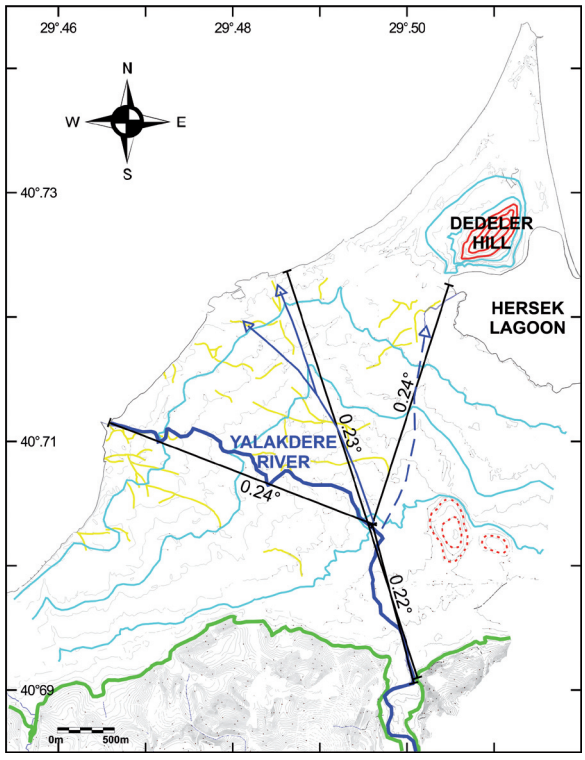

Fig. 2 - Topographic map of the Hersek Peninsula with elevation superimposed. In blue the Yalakdere River. The blue arrows represent old river directions as deduced from satellite data analysis (in yellow). The green line represents the approximated limit of the relief (15 m contour line); fair blue lines mark 5 m contour levels, while red lines represent contour levels above 10 m (5 m elevation interval). The slope calculated on different sections across the peninsula shows almost constant values between 0.22°-0.24° demonstrating a mature stage of the river evolution.

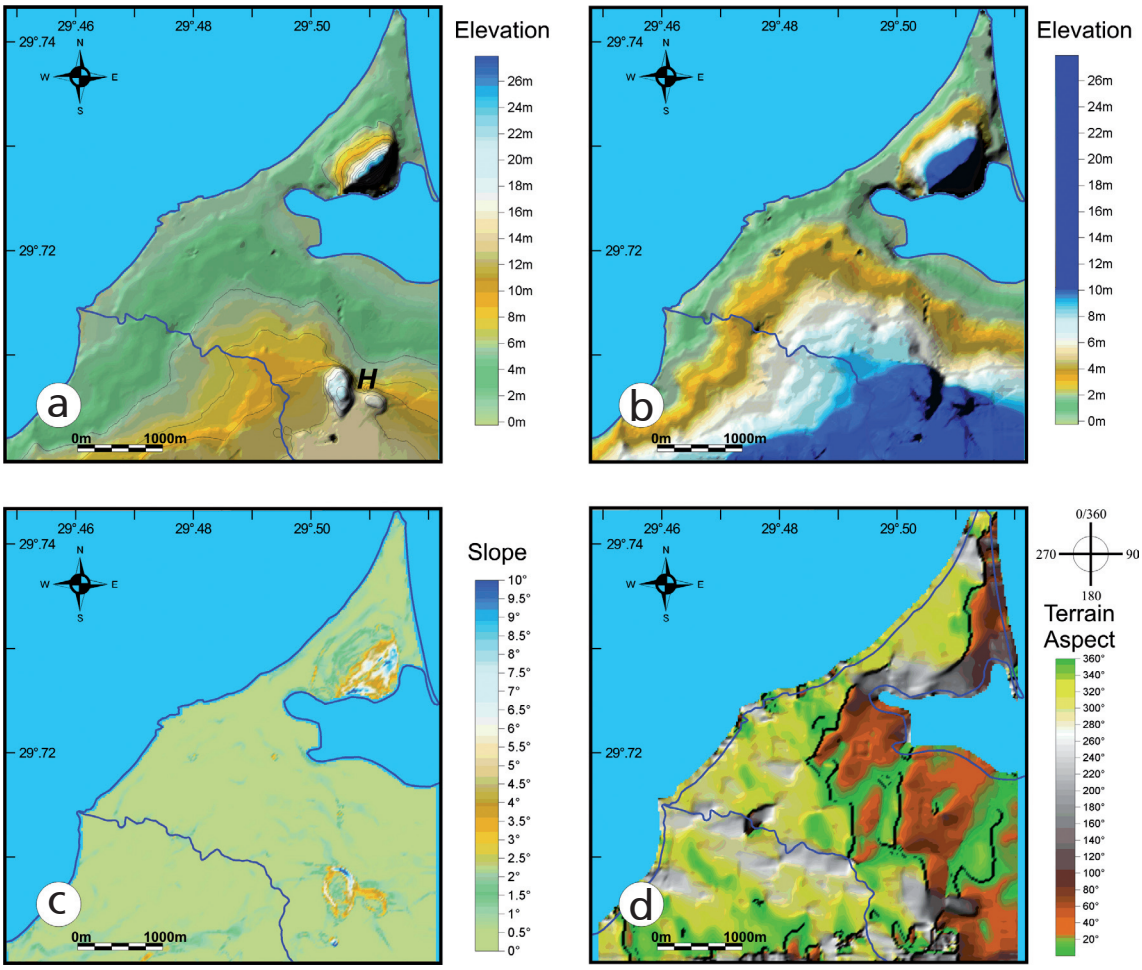

Fig. 3 - Topographic surface analyses obtained by processing 1:1000 data: a) DTM; b) DTM with a particular colour scale to enhance elevation differences. Despite small artefacts due to infrastructures and the not uniform original data sampling, the morphology of the delta lobes is evident; c) terrain slope; d) terrain aspect. The western portion of the plain has a mean slope direction towards NW, while the eastern part towards NE.

The fan-delta terrain slope is very uniform, with values around 0.23° (0.5%) also for the northern part of the gorge (Fig. 2). This feature and the meanders of the river suggest that it evolved and reached an advanced maturity. The southern segment of the Yalakdere is braided, while close to the springs it has a typical torrential flow with active erosion and high sediment entrainment.

The contour line shape (Fig. 2) and the shaded-relief rendering of the DTM (Figs. 3a and 3b) highlight the fan-delta morphology and the delta lobes suggesting a possible evolution of the system. The analysis shows:

a) a paleo river course with SE-NW direction and an old mouth located to the north of the present one;
b) a relatively recent migration of the mouth toward S-SW, probably through with several phases;

c) a possible old river course northwards, flowing occasionally into the lagoon, possibly during flood events;
d) a partial "barrage effect" during the delta progradation, due to two morphological highs in the south-western part of the plain: the sedimentation shadow zone is presently detectable to the north of the two hills (H in Fig. 3a).

The above inferences can be proved by the analysis of ground morphology obtained from airborne and satellite images. Fig. 2 shows the clearest paths related to the paleo-riverbed presenting a typical fan shape. In the western part of the delta, the terrain's aspect (Fig. 3d) has a mean value between 270°-320° while, in the eastern one, the main trend is from 15° to 50°. Such data are compatible with an evolution of the delta during two different phases: 1) a present-day phase, characterized by progradation towards west and NW; and 2) a previous phase, where progradation of the delta was mainly towards NE. The time sequence of the two phases is confirmed by the analysis of cores sampled in the Hersek lagoon at a maximum depth of 4 m. The stratigraphic analysis of these cores shows that at least during the last 2000 years (core bottom), the sediments of the lagoon originated exclusively from the sea, not forming the Yalakdere paleo-river and are related to silting up, shallowing upward deposits (Bertrand *et al.*, 2011).

2) Hersek lagoon

In the north-eastern part of the Hersek Peninsula there is a lagoon called the Hersek lagoon or Hersek lake. It is separated from the sea by a partly vegetated sandbar ranging in width between 5 and 50 m, and with a maximum elevation above the mean sea level of approximately 2 m. During violent sea storms, this coastal bar is submerged by water, especially along its thinner and shallower parts. The maximum E-W and N-S dimensions of the lagoon are similar, reaching 1.4 km; the total area is about 2 km^2. The western limit of the lagoon is not clearly defined, as it is marked by a marshy zone, with short channels and halophyte vegetation. The maximum water depth does not exceed few metres.

3) Dedeler Hill

Dedeler Hill is located to the north of the Hersek lagoon and it exhibits a maximum elevation of 28 m. Its dimensions are about 800 m and 450 m, measured in the NE-SW and NW-SE direction respectively, by considering the 10 m contour line as the limit. The main axis of the structure has a N48°E strike. The southern flank is characterized by steeper slope (mean value in the range 8°-10°), being slopes generally less than 5°, with a very gentle slope especially toward the coast.

2.2. Geology of the Hersek Peninsula

The oldest rocks outcropping in the Hersek Peninsula are classified in the Marmara formation, known as Altınova, in the vicinity of Karamürsel (Paluska *et al.*, 1989; Emre *et al.*, 1998; Yaltırak, 2002; Çağatay *et al.*, 2003). This formation includes marine terraces deposited at different sea levels during the Tyrrhenian period (Paluska *et al.*, 1989; Sakınç and Bargu, 1989; Görür *et al.*, 1997). Offshore seismic data show a unit that can be correlated with the upper portion of the Marmara (Altınova) formation corresponding to a major lowstand period, approximately at the end of the Last Glacial Maximum [around 12.5 kyrs: Alpar and Yaltırak (2002)].

Marmara formation's rocks crop out on Dedeler Hill (Fig. 4), but are normally concealed by vegetation. Rocks of the same formation were observed in trenches dug for the study of paleo-

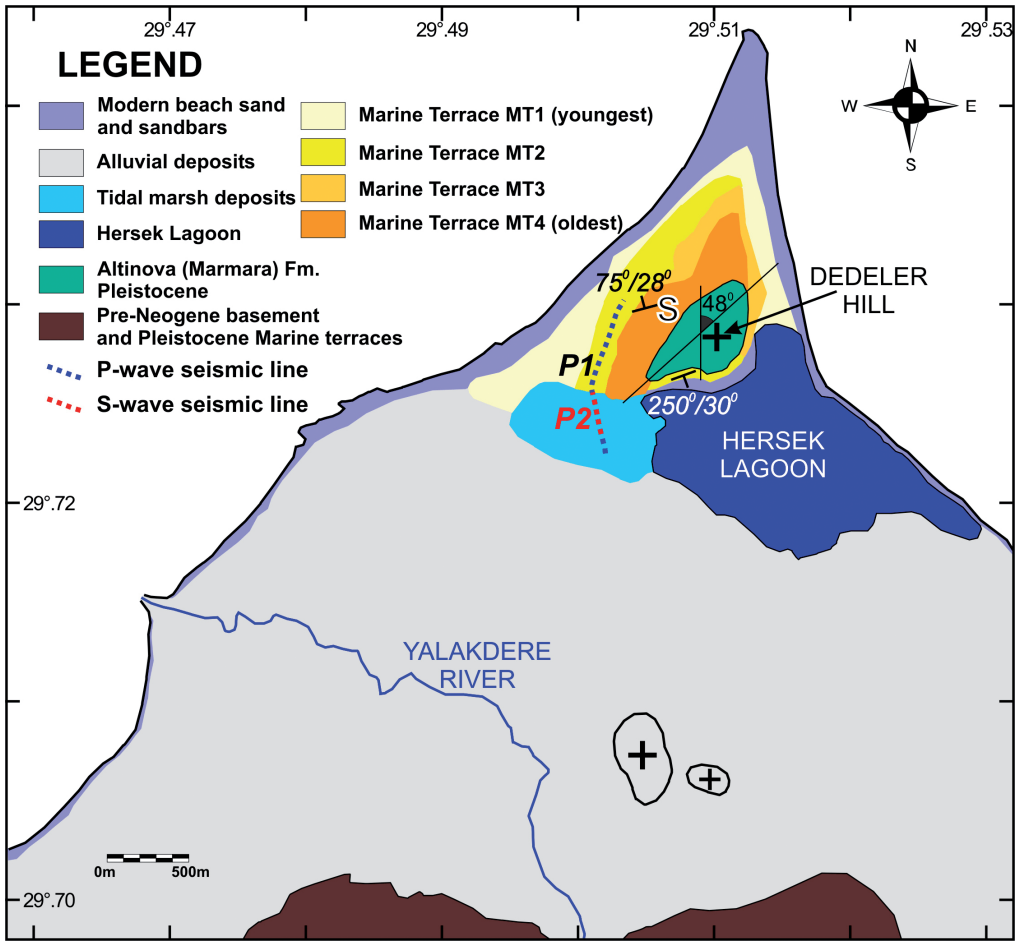

Fig. 4 - Schematic geological map of the Hersek Peninsula with superimposed the location of seismic profiles P1 and P2. The strike and dip at point "S" represent mean values referred to layers outcropping at an excavation for building foundations (summer 2006) (modified and integrated from Witter *et al.*, 2000; Lettis *et al.*, 2002; Özaksoy *et al.*, 2010, Kozaci *et al.*, 2011).

seismicity in the area bordering on the hill to the SW (Witter *et al.*, 2000).

At least 4 orders of Holocene marine terraces (Fig. 4) were identified around Dedeler Hill (Özaksoy *et al.*, 2010). The oldest terrace surface is about 7-8 m above the current sea level and extends to the west of the hill, while the youngest one surrounds the whole hill, but the southern side, with an elevation of about 2 m above the current sea level. All the terraces are most probably linked to co-seismic compressive phenomena with uplift rate of a few metres in the case of major earthquakes occurred in the Hersek zone. This hypothesis is confirmed by terrace tilting: the oldest terrace has a maximum 16° slope and the youngest one about 3°-4°. The 1600-2000 years old man-made structures exhibit a maximum 3° tilt (Witter *et al.*, 2000), demonstrating a strong tectonic activity also in very recent times.

The analysis of an outcrop in a large excavation (summer 2006; see Fig. 4 letter "S" for location) allowed us to reconstruct the stratigraphic sequence for the northern part of the Hersek Peninsula (Fig. 5).

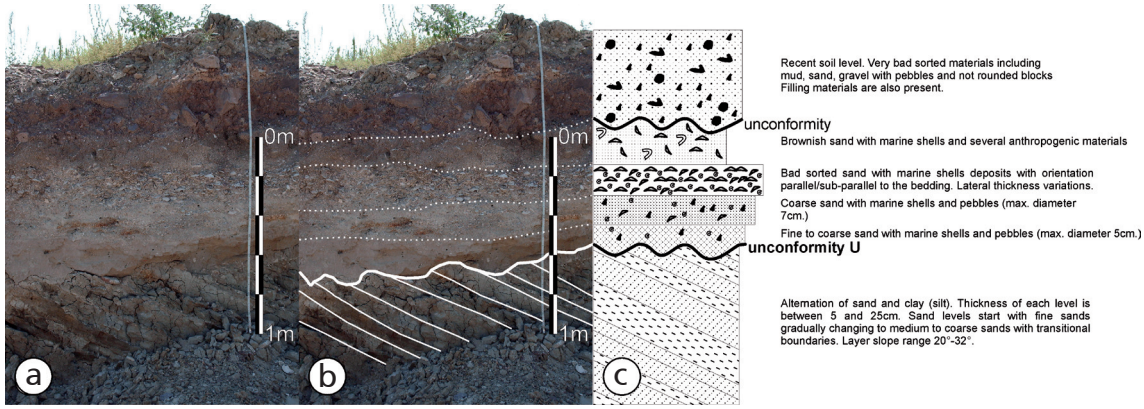

Fig. 5 - Litho-stratigraphic section deduced from a representative outcrop at the excavation point "S" of Fig. 4. A main unconformity "U" marks the hiatus between alternated and tilted sand and clay layers (bottom) and sands (top) and corresponds to the Late Glacial Erosion surface (about 12 kyrs B.P.): a) photograph of the outcrop; b) photograph of the outcrop with the stratigraphic limits superimposed; c) lithostratigraphic section.

In the deepest part of the trench there is an alternation of sand and clay with silt, similar to the situation observed in other trenches dug for paleo-seismic purposes around Dedeler Hill (Özaksoy *et al*., 2010). Strike and dip are quite variable, also because of the material plasticity, but the mean values are 75° and 28°, respectively. Silty levels are coarsening upwards from fine sand at the bottom to coarse sand at the top of each level, showing a general sea regression phase with possible climatic pulses. No macrofossils were found within sandy and clayey levels. This unit is topped by a clear erosion surface with the above levels settled as an unconformity.

The unit dates back to Upper Tyrrhenian as the outcrops observed at a road cut, to the east of the Topçular port (Çağatay *et al*., 2003). It is connected to climate variations of the late glaciation. The erosion surface probably formed during the low water level of the Marmara lake, around the end of the last glacial phase (about 12.5 kyrs B.P.). Post-transgression mud units, sand levels containing anthropogenic materials and coarse marine sediments deposited on the unconformity (Fig. 5).

2.3. Onshore tectonic structures around the İzmit Gulf

Two main sets of faults are interpreted in the Armutlu Peninsula to the south and in the Kocaeli Peninsula to the north, oriented NE-SW and NW-SE, respectively (Emre *et al*., 1998; Kuşçu *et al*., 2002; Alpar and Yaltırak, 2002; Dolu *et al*., 2007). The first set is clearly visible in the Armutlu Peninsula, to the south of the İzmit Gulf (Karamürsel and Yalova faults crossing the southern limit of the Hersek Peninsula), while the other system is more developed to the north of İzmit and in the region of the Çınarcık resort [e.g.: Termal and Orhangazi faults, Emre *et al*. (1998)]. Oversteps, splays and bending of the faults show up at different scales and give rise to ridges and troughs. Earlier studies propose rather simple tectono-kinematic schemes, such as the development of the gulf as a series of grabens (Crampin and Evans, 1986) or the existence of a single main normal fault (Saroglu *et al*., 1987). A model combining series of pull-apart basins was successively implemented, for the Marmara Sea (Barka and Kadinsky-Cade, 1988) and for the İzmit Gulf (Barka and Kuşçu, 1996; Armijo *et al*., 2002). Models based on pull-apart basins indicate that the slip is distributed between overlapping strike-slip segments.

2.4. Offshore tectonic structures within the İzmit Gulf

Fig. 6 shows the integration of the DTM of the Hersek Peninsula obtained using onshore topographic data and the sea-floor depth and offshore tectonic scheme inferred by Polonia *et al*. (2004) and Cormier *et al*. (2006); such structures are critically discussed hereafter.

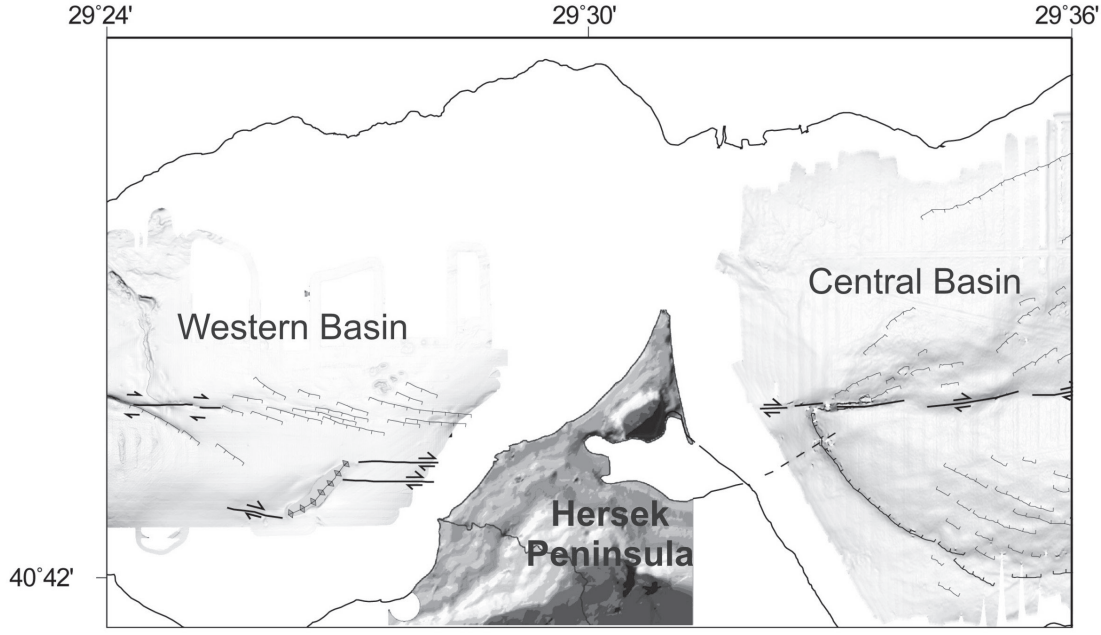

Fig. 6 - Onshore DTM and sea bottom morphology around the Hersek Peninsula data integration. The tectonic structures indicated refer to the interpretation of Polonia *et al*. (2004), Ferrante (2005) and Cormier *et al*. (2006).

2.4.1. Western Basin

A submarine canyon connects the western continental shelf of the İzmit Gulf to the Çınarcık Basin.

The major NAF deformation zone appears narrow and focused towards the basin west edge, while it shows a complex pattern of secondary splays and oversteps (Polonia *et al*., 2004; Cormier *et al*., 2006). Where deformation is more focused, the fault traces exhibit an E-W strike (N94°E), while in other zones the faults present a morphological expression, and a vertical dip toward east (Fig. 6).

In the Western Basin, from the analysis of the same seismic data, Kuşçu *et al*. (2002) locate other faults along the northern limit of the basin, while Gökaşan *et al*. (2001) identify a very complex fault system, partially reaching the sea floor and connecting at depth to form a flower structure close to the centre of the basin with other fault branches along the borders. Many authors suggest that the fault splits into two branches north of the Çatal delta: the main branch continues with an approximate E-W strike, while the second one bends to SE (Alpar and Yaltırak, 2002; Çağatay *et al*., 2003; Polonia *et al*., 2004; Cormier *et al*., 2006; Gasperini *et al*., 2011). The two faults are evident in the sea floor morphology, generating two scarps with N270° e N120° strike and south and SW dip, respectively.

Close to the Hersek Peninsula, the northern fault branch is divided into many *en-echelon* segments separated by a few hundred metres, ranging in length between 1 and 2 km, striking N104°E (±5°) and dipping towards SW (Fig. 6). Such faults were interpreted as Riedel shears surfacing above the main fault, or associated with sediment fluidization structures (Cormier *et al*., 2006). The *en-echelon* faults cut the sedimentary sequence and produce steps less than 1 m high at the sea floor (Gasperini *et al*., 2011). The southern strand is more discontinuous, showing NW-SE *en-echelon* fragmentation and connecting near Hersek with an E-W fault segment.

Many other structures were identified by means of geophysical surveys performed in the Western Basin, such as topographic highs and/or mud volcanoes. The larger one is a high located about 2.5 km to the west of the present mouth of the Yalakdere River. It is 1200 m long and about 300 m wide, rising about 40 m from the surrounding floor and reaching a minimum depth of about 35 m below the mean sea level (Polonia *et al*., 2002; Çağatay *et al*., 2003; Gasperini *et al*., 2011). This structure lies on the extension of the southern fault above described: it has a direction close to N45°E and maximum dip of the flanks reaching 15°. E-W fault branches border and cut both the northern and southern sectors. The interpretation of such major structure is not univocal, since it has been defined a "structural high" and a "paleo-island" (Polonia *et al*., 2004), a "pressure ridge" (Çağatay *et al*., 2003), a "seamount" (Kuşçu *et al*., 2002) or a "mud volcano" (Cormier *et al*., 2006; Kurt and Yücesoy, 2009).

The available geophysical data do not provide clear information about the inner structure of this high, because the maximum penetration depth of high-resolution seismic profiles does not exceed a few metres below the sea bottom. However, stratigraphic analysis of some gravity cores collected at the top of the structure (Çağatay *et al*., 2003; Polonia *et al*., 2004) suggests a tectonic origin of the high, connected to a local transpressional regime. Lacustrine units, which should normally be present at depths greater than –85 m, are observed at about –44 m of depth. This might indicate a tectonic uplift of more than 40 m during the last 12 kyrs. With similar considerations, Polonia *et al*. (2004) estimated a mean uplift value of 4-5 mm/year along the pressure ridge.

Smaller features (with a few hundred metres maximum width and 4-5 metres elevation above the surrounding sea floor) were detected along the previously described *en-echelon* fault system and were classified without adding further details as "mounds" (Polonia *et al*., 2004) or as "mud volcanoes" (Cormier *et al*., 2006).

2.4.2. Central (Karamürsel) Basin

The most outstanding element emerging from the bathymetry of the Central Basin (Fig. 6) is an escarpment, up to 90 m high, having a general E-W trend and, in more detail, striking N86°E in the western part, bending to a N97°E orientation in the eastern part, and bordering the northern flank in the middle of the basin (Cormier *et al*., 2006). The shelf is narrow in the southern sector, connecting the basin with a scarp, with an overall N130°E strike and ENE dip. In the central part, it runs almost parallel to the coastline and dips to NW. Some authors indicate that the main active fault in the Central Basin borders the southern limit of the depression close to the centre of the basin (Alpar and Yaltırak, 2002). This fault is interpreted as being formed by several interconnected right-stepped segments WNW-ESE oriented, with development of small pull-apart basins (Dolu *et al*., 2007). Other authors, using co-seismic land displacement measurements acquired after the 1999 seismic events, suggest that the main active

fault lies to the south of the area, along the coastline in the Karamürsel zone, and reaches the northern branch in the western basin (Barka *et al.*, 2002; Lettis *et al.*, 2002). Based on several geophysical data, the main fault segment is located along the northern border of the depression, at the centre of the basin (Kuşçu *et al.*, 2002; Çağatay *et al.*, 2006). Some authors suggest that many fault branches are intersecting the sea floor and emphasize the rheological differences between surface sediments and underlying basement (e.g., Gökaşan *et al.*, 2001), while others suppose that the NAF reaches the sea bottom only with few active segments (e.g., Kuşçu *et al.*, 2002) or even with a single main segment, locally characterized by *en-echelon* faults (e.g., Cormier *et al.*, 2006).

2.4.3. Hersek Peninsula

Clear surface evidences of fault segments crossing the Hersek Peninsula are not visible and not reported in literature. This fact could be related to the actual lack of tectonic structures (or to the presence of structures not reaching the topographic surface), but it could also be related to the rheological behavior of surface materials, namely incoherent sediments having various origin and composition. In fact, the morphology of the southern flank of the Dedeler Hill (scarp) could be interpreted as a fault plane, even if erosion and vegetation make this hypothesis difficult to prove. Moreover, paleoseismic trenches excavated into the peninsula at different positions do not provide conclusive evidence about position and recent activity of the faults (Witter *et al.*, 2000; Kozaci *et al.* 2011). The interpretation of trench data is further complicated by stratigraphic features, which are often mixed with the results of human activities.

Özaksoy *et al.* (2010) analyze the peninsula's uplifted marine terraces and use sedimentology, geomorphology and radiocarbon dating to recover the record of paleoseismic events. They calculate an elevation of the Hersek ridge 13 m above sea level around 2250 yrs B.C. and therefore a local uplift rate of 3.5 mm/yr over the last 4250 yrs, based on the location of the highest recognizable paleoshoreline terrace.

After the 1999 seismic events, many studies aimed at mapping the position and the amount of dislocations occurred on land. The easternmost surface displacement documented on land occurs in the Gölcük area, where the right lateral slip reached 5 m, with a vertical (normal) maximum displacement of more than 2 m (Lettis *et al.*, 2000, 2002; Barka *et al.*, 2002; Emre and Awata, 2003).

On the Hersek Peninsula there is no evidence of large surface ruptures due to the 1999 earthquakes. Nevertheless a crack zone with several centimetres of right lateral displacement was reported to the west of the Hersek lagoon. A co-seismic subsidence of about 20 cm occurred in the same area but it was rebounded in about two months after the 1999 event (Lettis *et al.*, 2000, 2002). Lateral spreading related both to the 1894 and to the 1999 events was also reported in the zone of the present Yalakdere mouth (Lettis *et al.*, 2000) with extensive liquefaction phenomena on the Hersek Peninsula (Ambraseys, 2001).

On land, other significant strain features were observed to the west of the Hersek Peninsula, on Çatal delta with a set of *en-echelon* extensional cracks, striking E-W on average (Barka *et al.*, 2002). There is no evidence of remarkable displacements, with the exception of the cracks of several down-to-the-north steps, having a maximum height of about 30 cm (Gülen *et al.*, 2002; Awata *et al.*, 2003; Emre and Awata, 2003; Dolu *et al.*, 2007).

A precise knowledge of the length of fault that ruptured during a large earthquake (and the

geometrical parameter of fault surface) is a critical element for the production of a reliable seismic risk assessment in the zone.

Surface evidence of ruptures and strain to the west of the Hersek Peninsula is discontinuous and not clear on land, but the distribution of the 1999 earthquake aftershocks shows epicentres aligned along a rather narrow zone, approximately trending E-W, with depth reaching 40-50 km to the west of the Hersek Peninsula (Wright *et al*., 2001; Karabulut *et al*., 2002; Polat *et al*., 2002; Bohnhoff *et al*., 2006). Such distribution suggests a release of seismic energy from a fault segment or a series of faults about 140-160 km long, i.e. including the rupture within the Western Basin (Fig. 1b). Recent submarine surveys by ROV, coupled with ultra-high resolution bathymetric data acquisition, actually detected sea floor fault traces, highlighted by scarps that reach a maximum height of about 50 cm (Gasperini *et al*., 2011; Uçarkuş *et al*., 2011). Previous bathymetric data were unable to resolve seafloor displacements to the west of the Hersek Peninsula and indicated that the slip along the fault surface decreased to an insignificant level to the west of Hersek. Moreover, the recent data evidenced displacements of the submarine canyons far from Hersek and reaching, or possibly crossing, the Çınarcık Basin (Armijo *et al*., 2005; Carton *et al*., 2007). Such observation is consistent not only with the rupture length suggested by the aftershocks but also with results of synthetic aperture radar (SAR) interferometry (Armijo *et al*., 2000; Wright *et al*., 2001; Çakır *et al*., 2003) and GPS data (Reilinger *et al*., 2000; Flerit *et al*., 2003). In addition, indications of the seismic data along the western shores of the Hersek Peninsula show active faults cutting the sea bottom, which indicate recent displacements and probable activity during the 1999 events (e.g. Alpar, 1999; Alpar and Yaltırak, 2002; Gasperini *et al*., 2011).

3. Methods

We acquired multi-fold reflection seismic data and we implemented synthetic models to estimate the deformations related to different tectonic scenarios and to gain insight into the role played by the Hersek Peninsula in the tectonic framework of the area. A key issue is to understand whether the lack of major deformations on the Hersek Peninsula is due to: 1) a seismic gap; 2) a relatively small displacement not able to produce surface ruptures within soft and plastic deltaic sediments; 3) the geometry of the faults, which on land is actually unknown and only tentative correlations are made (e.g., Bertrand *et al*., 2011; Kozaci *et al*., 2011), 4) a combination of such different causes.

The reflection seismic survey aims at obtaining information on the structural, stratigraphic and tectonic setting, while the synthetic deformation models aim at verifying the compatibility of the present Hersek delta's morphology with the tectonic model emerging from land and offshore data integration.

3.1. Seismic data acquisition and processing

We acquired two seismic profiles, 1031.25 m (401 shots) and 378.75 m (189 shots) long, respectively (Fig. 7). Both profiles were recorded using a Geode seismograph (Geometrics). We used a 5 kg sledgehammer as energy source for profile P1, with vertical impact on a metal plate and 24 vertical geophones with 14 Hz natural frequency, basically recording the compressional

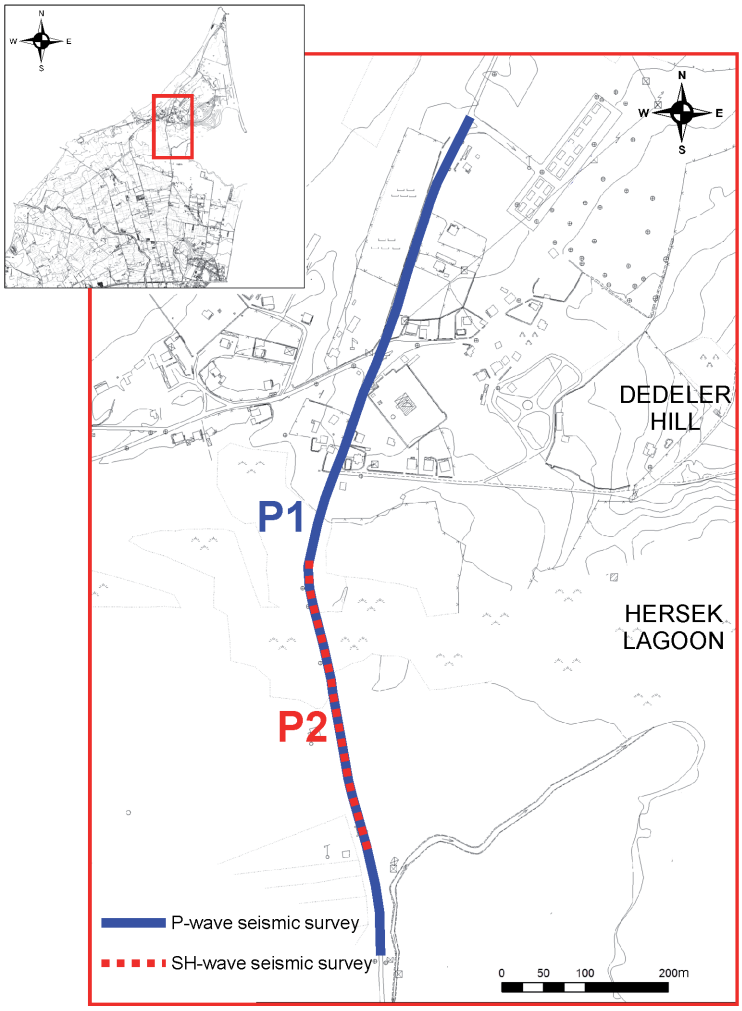

Fig. 7 - Detailed location map of seismic profiles P1 and P2.

(and Rayleigh) wavefield; 4 hits per each source point have been used to reduce random noises. We set the following acquisition geometry after analysis of the walkaway tests: 2.5 m geophone interval, 2.5 m shot interval and minimum offset (maximum offset 60 m) to obtain a maximum 1200% fold with 1.25 m CMP spacing.

We decided to integrate the P-wave section with S-waves acquisition, to improve imaging and resolution in the shallow part of the section, and to gain further insight into characteristics of subsurface materials through the joint analysis and comparison of P and SH wave velocities. For this aim, a segment of profile P1 was further surveyed (P2 hereafter) by using the same seismic source, but striking horizontally a weighted H shaped steel bar fixed to the ground with metal nails (total weight of 100 kg). We used horizontal geophones to record shear waves (SH). In this case we used 18 horizontal geophones with 10 Hz natural frequency with the following geometry: 2.5 m geophone interval; minimum offset and shot interval equal to 2.5 m to obtain a maximum 900% fold and 1.25 m CMP spacing (maximum offset equal to 45 m). Two shots with opposite impact directions were obtained at each shot point location.

This is the first high-resolution two components seismic survey acquired on the Hersek Peninsula (see also Forte *et al.*, 2009). Recently, Kozaci *et al.* (2011) published a 650-m long seismic profile acquired using 12 recording channels and 30 shots, obtaining therefore a very low-folding section. This profile shows a two-way traveltime shorter than 50 ms and no processing/analysis details are provided.

The processing sequence applied to seismic profile P1 (P-waves) is summarised in Table 1.

Table 1 - Seismic processing flow.

Application order	Processing steps
1	Geometry definition
2	Editing and preprocessing
3	Spectral and f-k analysis
4	Amplitude analysis and recovery
5	Filtering
6	Ground Roll (Rayleigh waves) removal
7	Semblance velocity analysis
8	Stacking
9	Post-stack Kirchhoff migration

The amplitude decay analysis and recovery were a crucial step for the subsequent phase of data interpretation. We applied a true-amplitude processing to preserve original contrasts and to use them as an auxiliary parameter for the interpretation. Original data exhibit an overall high coherent noise level due to Rayleigh waves (usually referred as ground-roll), which undergo a lower attenuation compared to body waves and hinder the identification of the reflected wavefield. The application of filters implemented in the f-k and τ-p domains allows the selective removal of such component.

A similar processing sequence was applied to the shear waves profile (P2) as well, with some additional steps: during the pre-processing phase the shots obtained at the same shot point with opposite impact direction were subtracted to stack in phase the SH wavefield. The other components (such as SV and P waves) were cancelled out or largely attenuated by such operation (see e.g., Garotta, 1999).

No static corrections were applied to both profiles since the maximum measured elevation difference is about 2.5 m with a very small gradient and no detectable effect on reflection times.

3.2. Structural modelling

We employed Coulomb 3.0 program (Lin and Stein, 2004; Toda *et al.*, 2005) to model the tectonic deformation with the finite elements method. Calculations are made in elastic half-space with uniform isotropic elastic properties. In this study we focused on the estimation of the percent partitioning between horizontal and vertical displacements, determining the effects produced on the surface by different partitions of a pure strike-slip movement along several modeled fault planes. We set a half-space with constant depth of 5 km as model background, latitude between

40.68°N and 40.76°N, and longitude between 29.35°E and 29.60°E, to obtain a resolution level comparable with the results deduced from the geological, geomorphological and geophysical analyses. The approximated linear dimensions are about 9 km and 21 km in N-S and E-W direction, respectively. We set the following half-space rheological parameters: Young modulus 800 kbar, Poisson ratio 0.25 and friction coefficient 0.4. The cell size is 200 m by 200 m.

We ran simulations to evaluate vertical and horizontal displacements produced by different fault configurations, calculated on a zero depth surface (i.e., on mean sea level) or on vertical sections.

4. Results

4.1. Seismic data interpretation

The P-wave stacked section (P1 in Fig. 8) provides important and new information about the subsurface stratigraphy and structural/tectonic setting. The maximum signal penetration depth is about 400-500 ms (two-way traveltime), particularly in the southern part of the section where highly reflective contacts show up in the sedimentary sequence. In the northern part, the global reflectivity is lower and also the lateral coherency of the reflectors decreases.

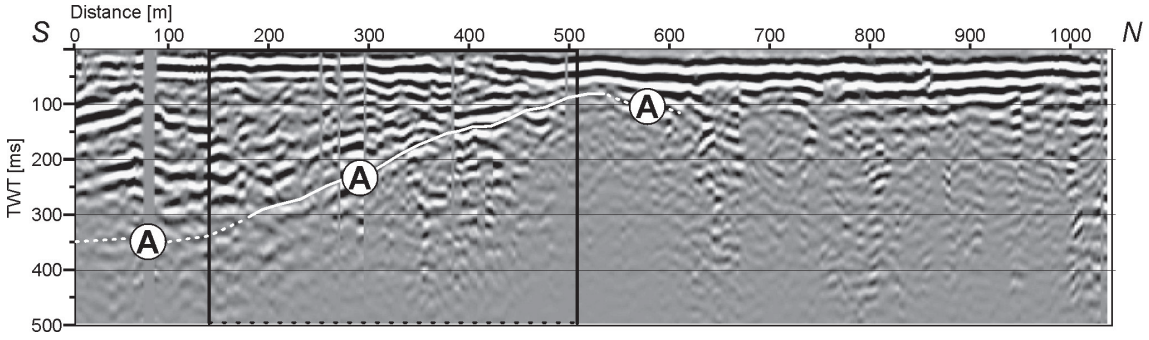

Fig. 8 - Stacked section of seismic profile P1. Several layers terminate in onlap on the deepest interpretable horizon-A. The black frame represents the portion of profile P1 corresponding with P2.

From the seismic section shown in Fig. 8, we observe that several dipping reflectors onlap a basal horizon (A). In the northern part of the section, between 500 and 700 m, reflectors dip antithetically to those observed in the southern sector. Such variations are further highlighted by the stacking velocity field (Fig. 9). We performed a binning between adjacent CMPs to obtain more detailed information on the seismic velocities. The resulting reflection point error is negligible, since it is namely 1.25 m. It is thus possible to improve the velocity analysis by calculating the semblance (or other coherency functions) on bins having 2400% and 1800% fold along profiles P1 and P2, respectively.

We checked and edited the resulting velocity field to verify interval velocities and to remove unrealistic lateral and vertical variations. The shallow part (between about 0-200 ms) is characterized by average P-wave velocities up to 700 m/s. Lower values of 570 m/s are observed

in the first 150 m of the seismic profile, while the velocities are higher (750-800 m/s) in the zone between 200 and 450 m. A rather sharp velocity increase, with values higher than 800 m/s, occurs beneath the described levels. All these values are quite low, which is in agreement with young unconsolidated sediments. The mean Vp/Vs ratio is within 2-2.5 range.

The higher velocity gradient follows the previously described horizon (A) and confirms the presence of an active fold related to a compressive deformation pattern. Profile P1 (Figs. 8 and 9) is characterized by several phase variations. Although it is not possible to easily correlate them with tectonic discontinuities, because the data resolution makes impossible to define significant fault throws, we cannot exclude that they mark sub-vertical fault planes.

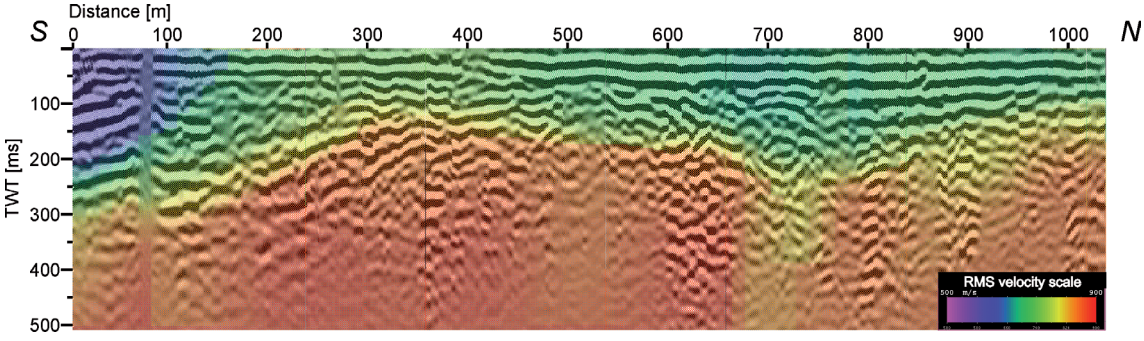

Fig. 9 - Stacked section of seismic profile P1 with RMS velocity field superimposed.

Fig. 10 shows the profile P2 stacked section, from shear waves survey. The S-wave section shows an overall enhanced resolution (if we consider the same frequency range), due to the lower velocities. It is so possible to image structures beyond the resolution of the P-wave profile. The horizon-A is clearly outlined and exhibits an average dip around 15°. The onlap terminations over "A" are unambiguous as well as the dip of the layers, tending to zero as they approach the topographic surface. Such behavior demonstrates a syn-sedimentary tectonic deformation. The S-wave section evidences also sub-vertical discontinuities (α and β in Fig. 10) that are not clearly imaged in the P-wave section (Figs. 8 and 9). Such geometries are not consistent with a fan-delta progradation from south, but rather with a push-up produced by active compressive tectonic. In the Hersek zone there are no useful boreholes to calibrate seismic stratigraphy, with the exception of one located at the northern tip of the peninsula, about 1500 m off the northern end of seismic profile P1. This borehole reaches a 118.45 m depth and does not cross the carbonate basement located at a depth of about 20-40 m within boreholes drilled close to the northern coast of the İzmit Gulf (Çetin *et al*., 1995; Ediger and Ergin, 1995; Meriç *et al*., 1995). However, based on the study of the trench to the east of the seismic profiles (Fig. 4) and on the stratigraphic correlations (Fig. 5), horizon-A can be interpreted as the late glacial erosion surface unconformity.

The dips and attitudes obtained from seismic sections are actually in agreement with structural data obtained from the trenches. Also, the reflectivity contrasts are consistent with the observed lithological contacts. The erosion surface related with horizon-A was identified also offshore, using high-resolution seismic data. It consists of a very sharp reflector marking a geometrical unconformity between the upper transparent levels deposited since the beginning of the Holocene

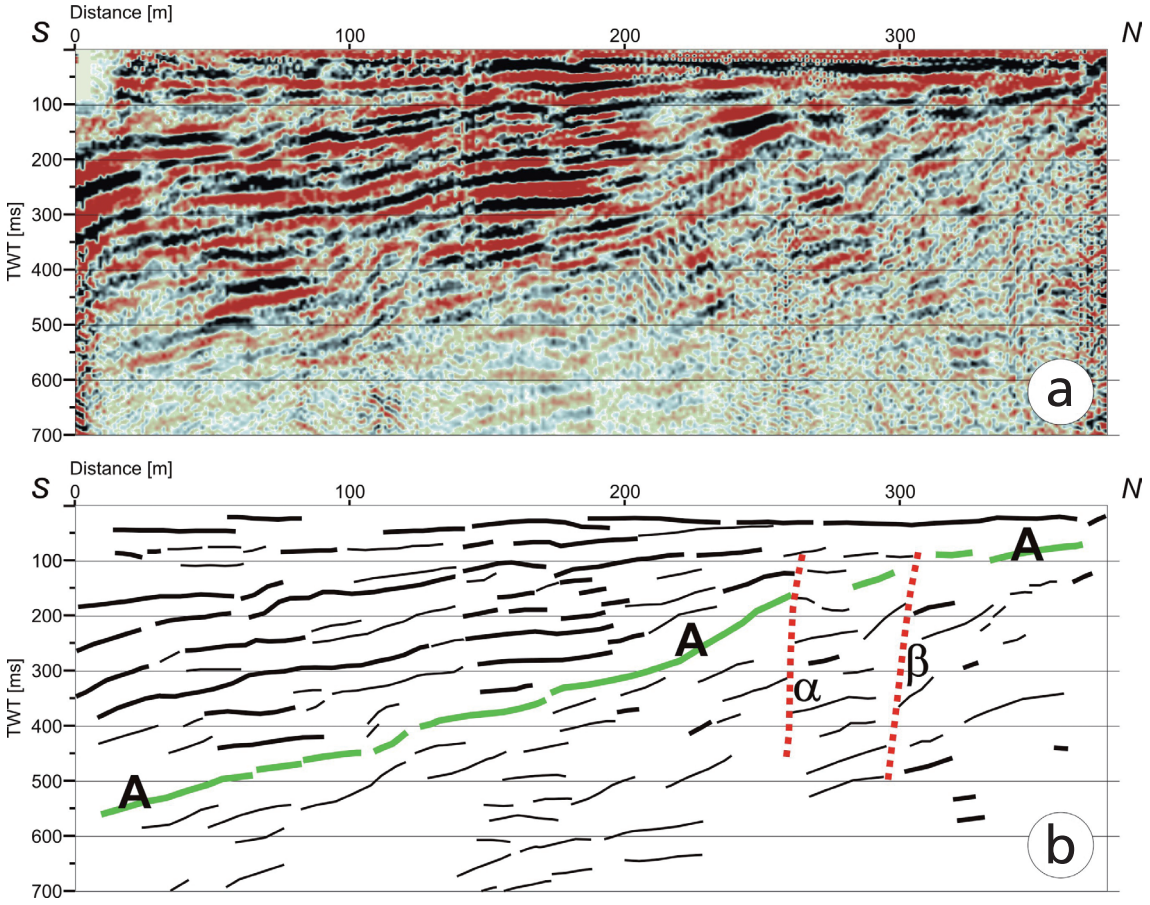

Fig. 10 - a) Seismic profile P2: stacked section (S-waves); b) line drawing. Green line corresponds to horizon-A in Fig. 8. (α) and (β) indicate possible fault locations. See text for interpretation details.

and the lower, more reflective deposits dating Late Pleistocene (Alpar, 1999; Gökaşan *et al.*, 2001, 2003; Kuşçu *et al.*, 2002; Alpar and Yaltırak, 2002; Çağatay *et al.*, 2003).

4.2. Crustal deformation and vertical displacement modeling

The observed transpressive deformations in the Hersek Peninsula could be caused either by stepovers or bends along the NAF system. There is not an agreement between these two "end members" proposed on the basis of marine geological data in literature; therefore we evaluated both vertical and horizontal displacements assuming fault segments deduced from the recent literature and running scaled models consistent with different tectonic scenarios.

We simulated the effects of a fault identified in several seismic marine data sets and reported in literature (Alpar, 1999; Kuşçu *et al.*, 2002; Çağatay *et al.*, 2003; Cormier *et al.*, 2006), striking N086°E to the east of the Hersek Peninsula. In the western basin we set a second N94°E fault (Fig. 6) that is an approximation and simplification of the sea floor situation where series of *en-echelon* faults were identified (Polonia *et al.*, 2004). Such two faults, making a restraining bend, were extended up to their intersection point located to the north of the Hersek lagoon, close to the base of Dedeler Hill (Fig. 11). We also simulated the effects obtained by

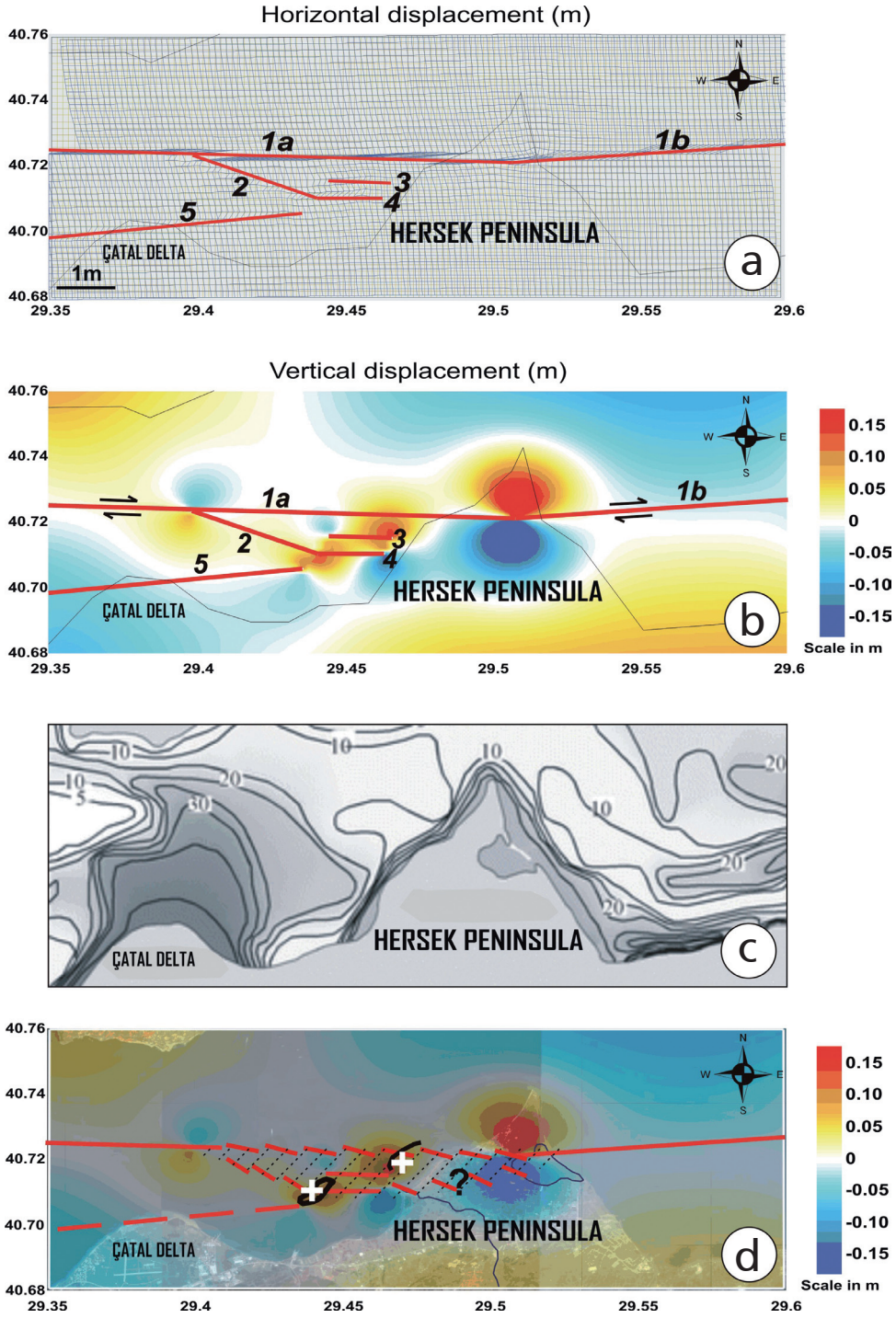

Fig. 11 - Crustal deformation and vertical displacement modelling: a) co-seismic horizontal displacement due to different pure strike-slip movements along fault segments 1a, 1b, 2, 3, 4 and 5; b) co-seismic vertical displacement (in metres) due to strike-slip movements as for (a); c) thickness of Holocene deposits (in metres) in a portion of the İzmit Gulf corresponding to the area used for modelling (from Dolu *et al*., 2007); d) vertical displacement model superimposed on the satellite image of the same area. In red, the inferred schematic fault pattern. The red dotted lines represent fault segments that are not visible at the surface or *en-echelon* zones both onshore and offshore. The dotted lines mark a lens connecting two or more fault branches into one fault segment towards east and west. The positions of submarine topographic highs are from Polonia *et al*. (2004) and Cormier *et al*. (2006).

the inclusion of other active fault segments of the western basin into the model that are located to the south of the branch above described. In detail, we considered a system composed by a southward bounding strike-slip fault at 29.4° longitude, with an average N114°E strike, and two active segments having approximated E-W direction (Fig. 11a). Due to the lack of published onshore seismic data we decided to not extend such fault segments up to the Hersek Peninsula. We defined also another strike-slip fault (strike N86°E) crossing the Çatal delta in the zone where many surface deformations have been identified after the 1999 seismic events (Barka *et al*., 2000, 2002; Gülen *et al*., 2002; Awata *et al*., 2003; Emre and Awata, 2003). This fault has been extended to 29.44° longitude according to the results of Kuşçu *et al*. (2002).

We extended all fault planes from the model surface to the bottom (5 km), assuming that all of them are vertical. Such a model is necessarily simplified, because the real geometry of the faults varies with depth in compliance with variations in rheological properties, and the fault surface is, in general, not planar. Nevertheless, it is an acceptable approximation to infer the displacements due to a pure strike-slip movement. Present land and sea bottom morphologies can be explained by stress/strain simulations performed on an assumed network of faults having a pure dextral strike slip co-seismic movement distributed as follows: 1 m along faults 1a and 1b, 15 cm along fault segment 2 and 10 cm along faults 3, 4 and 5 (Fig. 11a). In this analysis, the adopted horizontal displacement values are not the key factor and are not related to a specific seismic event because our aim is to estimate the partitioning between vertical and horizontal relative movements along different fault segments. Such a model shows strong deformations in the zone where the 1a and 1b branches join together, producing an uplift to the north and subsidence effects to the south, both reaching a value of about 15-20% of the strike slip movement (Fig. 11b).

The simulated maximum uplift area is in good agreement with the location of Dedeler Hill and the surrounding Holocene marine terraces (Fig. 11), while the subsidence zone corresponds, even if with less accuracy, with the lagoon that is probably created by tectonic subsidence as recently suggested by Bertrand *et al*. (2011) using detailed sedimentary analyses on core samples taken on different positions within the lagoon.

At the seafloor, the uplift zones (reaching maximum vertical displacement values of about 10% of lateral movement) are in quite good agreement with the location of the highs reported in literature (Çağatay *et al*., 2003; Polonia *et al*., 2004; Cormier *et al*., 2006; Gasperini *et al*., 2011). In particular, the area of uplift close to the eastern limit of fault number 5, can be related to the structure rising about 40 m above the surrounding sea floor, described and interpreted in different ways on the basis of several geophysical data sets (Kuşçu *et al*., 2002; Çağatay *et al*., 2003; Polonia *et al*., 2004). The morphology between faults 1a, 3 and 4 can be related to the structure described as "mud volcano" and localized only on the western flank. Shallow water conditions actually prevent the acquisition of geophysical data on the side towards the Hersek Peninsula (Fig. 11d). Simulation results suggest a tectonic origin for such structure, basically associated with local transpressive movements as in the case of Dedeler Hill. Another interesting feature is the area that exhibits compressional deformation along the *en-echelon* fault zone (central part of fault segment 1a in Fig. 11b) where the presence of mud volcanoes has been reported.

High subsidence values characterize the lagoon zone and the area close to the present-day mouth of the Yalakdere River, which probably migrated from north to SW (see also Figs. 2 and 3 and relative comments) because of topographic variations associated with tectonic movements.

The partition of the strike slip movement along different fault segments with a percentage of about 85-90% to the north and 10-15% to the south is in agreement with the results of Polonia *et al*. (2004) based on lateral displacement measurements of a submarine channel crossing the two fault segments: 80 m along the northern fault (segment 1a in Fig. 11b) and 10 m along the southern one (segment 2 in Fig. 11b). The same authors calculate a strike slip displacement rate along the northern fault of 10±1.5 mm/yr during the Holocene and suggest that the fault branch developed in this zone from the end of the Pleistocene – beginning of the Holocene (about 12 kyrs B.P.). Therefore the total lateral displacement is close to 120 m. The morphology of the northern tip of the Hersek Peninsula, i.e., the zone to the north of the fault, is compatible with a dextral shear movement. An average uplift rate for the Holocene about 3 mm/yr (Çağatay *et al*., 2003) and about 5 mm/yr (Polonia *et al*., 2004) was calculated for the elevated zones to the west of the Hersek Peninsula, while a value of 3.5 mm/yr was estimated for the last 4250 years by Özaksoy *et al*. (2010) analyzing the marine terraces uplift and the sediments within trenches. These values are comparable to those obtained from our numerical simulation (vertical movements of about 15-20% of the strike slip component).

Our seismic data sets show that Holocene sediments lay in onlap above the horizon interpreted as the late glacial erosional unconformity (A in Figs. 8 and 10). They show a variable dip, and an estimated maximum thickness around 75 m, based on P and S velocity values (Fig. 8). Therefore the minimum uplift rate is close to 6 mm/yr (75 m/12 kyrs), which is the same order of magnitude of the value calculated with different data on transpressive structures to the west of the peninsula and to the results obtained by Özaksoy *et al*. (2010). Moreover, if this fault activity started during the Holocene and we consider that the recurrence interval of major earthquakes in this area is about 200-250 years (Ambraseys and Finkel, 1991) and that the co-seismic uplift is about 2 m for each major event (Özaksoy *et al*., 2010), we obtain a total uplift referred to the last 12 kyrs of about 100 m, comparable with the other estimates. Using seismic data, we obtain a maximum 6 mm/yr sedimentation rate to the south of the main fault segment, a value comparable with the direct radiocarbon measurements on core samples from the lagoon [2-4 mm/yr: Bertrand *et al*. (2011)].

The comparison between our results and the thickness of Holocene deposits mapped using high-resolution marine seismic data (Dolu *et al*., 2007) suggests that the maximum values (i.e., the higher sedimentation rates) are found in the eastern and central part of the Hersek Peninsula, while in the western part the Holocene layers are thinner; here is where our model predicts the maximum uplift rate. The thickness of the sediments is higher to the SW of the peninsula, especially in the area located to the south of the present river mouth, where the model correctly predicts a subsiding area. Results of the numerical simulation show that maximum and minimum sediment thicknesses are related to subsiding and emerging sectors, respectively. The thickness of Holocene deposits rapidly decreases from about 40 m close to the coast, to 10 m offshore the delta (Figs. 11c and 11d).

5. Discussion

The integrated analyses of available geological, geomorphological and geophysical data, in conjunction with the interpretation of the newly collected seismic reflection profiles presented in

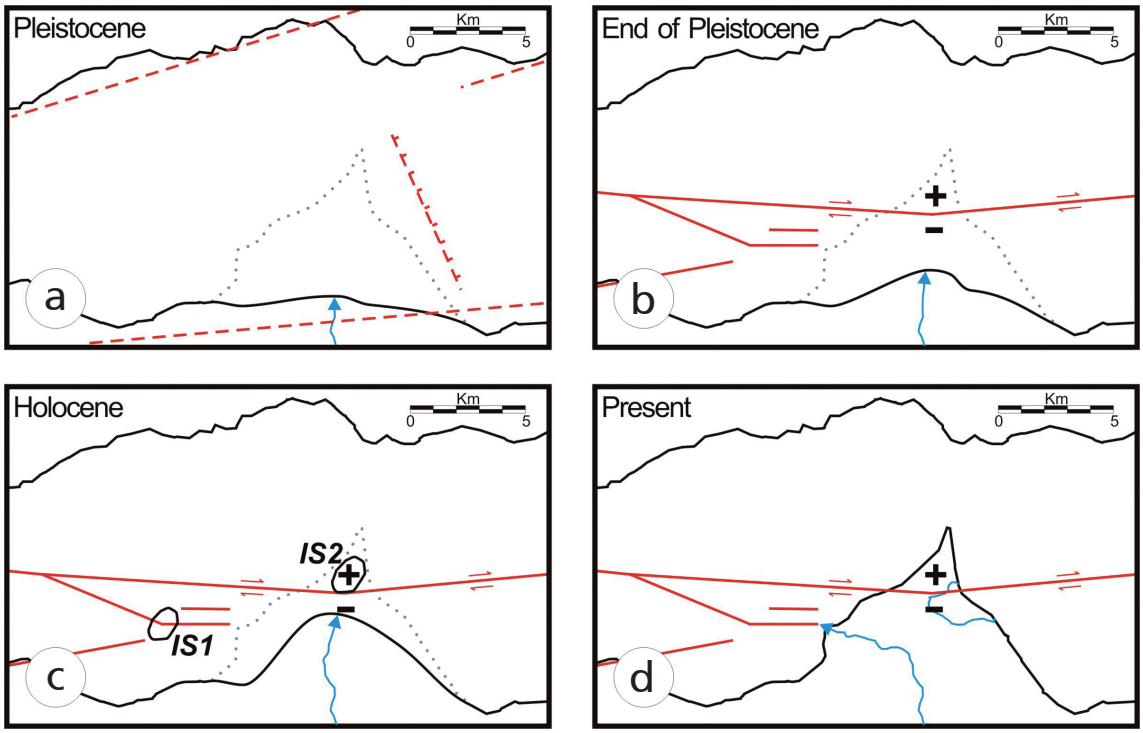

Fig. 12 - Schematic evolution of the Hersek Peninsula from the end of Pleistocene to Present: a) Pleistocene tectonic sketch based on Barka (1997), Emre *et al*. (1998) and Gökaşan *et al*. (2001). This tectonic situation was not considered in our study, since our models encompass a fault distribution developed in the late Pleistocene/early Holocene (b); c) IS1 represents a paleo island, presently below sea level, while IS2 corresponds to the current Dedeler Hill; d) present situation showing the Hersek lagoon in the still active subsiding zone and the present path/mouth of the Yalakdere River. The dotted black line marks the current border of the Hersek Peninsula. The paleo-river location is approximate because the scheme cannot consider all the sea level variations, which obviously produce large mouth changes.

this study, indicate that the Hersek Peninsula is a complex structure produced by the interaction between the prograding deposits supplied at the front of a fluvial delta, and a transpressive structural high produced by a remarkable uplift with morphological expression that culminates at the top of the Dedeler Hill. This structure, as well as the submarine highs surrounding the peninsula to the west, is NE-SW oriented, a clear evidence that such features are related to local transpression formed at a major bending (or a left-lateral small step) along a dextral strike-slip fault. Based on the reconstruction of this structural pattern, and on the study of all available geological information for this sector of the NAF, we propose the following scheme for the evolution of the Hersek Peninsula and surrounding areas (Fig. 12). The (Paleo) Hersek delta grew up with a relatively large sedimentary input due to the erosion and the widening of a gorge excavated in the Armutlu area as a consequence of the uplift of this peninsula. Its development was further affected by the currents in the paleo-basin (Alpar and Güneysu, 1999). During the late Pleistocene/early Holocene (Fig. 12b), a new fault developed (Polonia *et al*., 2004), producing in the present Hersek Peninsula area a restraining bend of about 8° with transpressive effects to the north and subsidence to S-SE. Within the Western Basin, the principal strike slip movement was accommodated by the new northern fault segment (85-90%), while to the south the deformation was split in more than one segment creating local transpression with an uplift rate ranging between 3 and 6 mm/yr.

Such kinematic conditions characterized the area in the subsequent period (Çağatay *et al*., 2003), leading to the formation of structural highs that during sea level lowstand periods reached the sea surface and emerged as islands (Paleo island IS1 in Fig. 12c).

Holocene marine terraces presently outcropping the Dedeler Hill north of the main NAF track roughly around the maximum bending point, indicate that this area emerged as a paleo-island (IS2 in Fig. 12c). The paleo Yalakdere River deposits (with the important contribution of marine currents) reached this island that was connected to land. Due to the lateral displacement along the NAF main strand, the location of the Yalakdere River changed, moving gradually toward west up to its present-day position (Fig. 12d). A recent stratigraphic analysis carried out on boreholes drilled into the lagoon shows that the sediments of the lagoon are marine during at least the last 2000 years (Bertrand *et al*., 2011). This implies that the area, although rapidly subsiding, has been never fed in this period by the Yalakdere River deposits. Such evidence can be explained taking into account the different distribution and effects of tectonic tilting. In particular, the increasing uplift of the northern portion of the present Hersek Peninsula created a barrier to further fluvial deposits. The delta plain underwent in this way a diversion toward N-NW. The sea level variations obviously played a crucial role in controlling the deposition rates, and we might suppose that the maximum developments of the delta coincided with the sea level low-stand, when the river base-level reached a minimum.

The two morphological highs visible south of the delta plain (Figs. 3 and 4) are most probably of tectonic origin, as is the case for the Dedeler Hill and for the other already described submarine structures, but this should be verified by other geological and geophysical data. Further geo-marine surveys are also required to obtain a complete dating of the sediments displaced by the faults crossing the Hersek Peninsula and provide a better-constrained kinematic scheme for the geological evolution of this peculiar feature.

6. Conclusion

Our study shows that the Hersek Peninsula was formed by the combined effect of a restraining bend (or a small stepover) along the NAF in the Gulf of İzmit, and the progradation of the Yalakdere River that reached a maximum during the last glacial time (12-14 kyr B.P.). This transpressive pattern, also observed in the submarine environment west of the peninsula, overprints the general transtensive tectonics observed in the rapidly subsiding *pull-apart* basins that form the İzmit Gulf. This might indicate a "focusing" of the principal deformation zone in the strike-slip fault system, that could have evolved from a relative wide shear zone characterized by large-scale stepovers and *en-echelon* faults systems, to a more localized and narrow principal deformation zone occurred in different steps starting from the end of Pleistocene and probably still in progress especially in the Western Basin. Numerical simulations and land seismic profiles supplied by the present study, integrated by previous geomorphological data, detailed bathymetric maps and marine geophysical surveys, suggest that formation of Hersek Peninsula is rather recent, probably dating back to not before than the Pleistocene and due to combined tectonic, fluvial and marine effects. In particular, considering the tectonic deformations and sedimentation rates calculated, the hypothesis of a Hersek Delta development in the early Pliocene (e.g., Alpar and Yaltırak, 2002) has been reviewed. On the

other hand, it is quite evident that sediments supplied by the (paleo) Yalakdere River, especially during the sea level lowstands at 150-130 and 24-12 kyrs, and the early deglaciation phases, allowed the progradation of the Hersek Delta (Alpar and Güneysu, 1999). Our reconstruction also suggests that deformation to the east of Hersek is presently concentrated in a relatively narrow zone, along one major fault segment, while to the west of the Hersek Peninsula (i.e., in the Darica Western Basin) distinct fault segments, within an area about 12 km long and 2 km wide, accommodate transpressive and transtensive strains. The compressive structures imaged by our seismic profiles in the northern part of Hersek constitute a widening of the principal deformation zone, were earthquake-related surface ruptures could not be easily identified. The combined reflection seismic data and synthetic modelling results, demonstrated that a restraining bend of about 8° centred on the Hersek Peninsula and originally proposed by Polonia *et al*. (2004) and by Cormier *et al*. (2006) just connecting offshore data, is consistent with the existing morphologies.

Furthermore, several compressive and extensive features are accurately modelled by partitioning the pure strike-slip movement into a single fault crossing the Central and Western basins (85-90% of total movement) and into a deformation of 10-15% along fault segments to the SW of Hersek.

Although our seismic profiles show vertical discontinuities that could be interpreted as fault planes, we cannot unequivocally identify heaves on our seismic sections. This effect could be related to the high coherent noise level (ground roll) in the original data, and to the relatively narrow frequency band of the source wavelet, causing a fairly poor resolution, but also to the existence of a series of short and not linked *en-echelon* segments, similar to those observed offshore west of Hersek, which are related to diffuse stress accommodation. Finally, deltaic sediments can also conceal the fault rupture due to the high plasticity of soils after the liquefaction phenomena that occurred in the Hersek Peninsula also during historical earthquakes.

The study area, despite its limited extension, is indubitably a key point for several reasons: it represents the only onshore segment of the NAF within the central part of the İzmit Gulf and it showed peculiar effects occurred during the 1999 seismic events. Therefore, is crucial to assess seismic risk and future earthquake scenarios through enhanced knowledge of space and time distribution of tectonic stresses in a region where important infrastructures as the new Istanbul-İzmit highway connecting the northern coast to Hersek are planned.

Acknowledgements. We gratefully acknowledge the support of the Italian Ministry of University and Scientific Research for funding through PRIN grant 2006 and of Halliburton through Landmark academic grant. We thank Cengiz Zabci and Namýk Çağatay of ITÜ-EMCOL (eastern Mediterranean Centre for Oceanography and Limnology, Istanbul Technical University) for support and helpful comments. The authors thank Giancarlo Dal Moro and Paolo Gabrielli for assistance in seismic data acquisition and Jung Ran Forte for the paper editing. Alina Polonia and Valentina Ferrante are acknowledged for some geomorphological and structural marine data presented. Giuliana Rossi and Alessandro Vuan are kindly acknowledged for their great help in improving the manuscript.

REFERENCES

Alpar B.; 1999: *Underwater signatures of the Kocaeli earthquake (August 17th 1999)*. Turkish J. of Marine Sciences, **5**(3), 111-130.

Alpar B. and Güneysu A.C.; 1999: *Evolution of the Hersek Delta (İzmit Bay)*. Turkish J. of Marine Sciences, **5**(2), 57-74.

Alpar B. and Yaltırak C.; 2002: *Characteristic features of the North Anatolian Fault in the eastern Marmara region and its tectonic evolution*. Marine Geology, **190**, 329-350.

Alpar B. and Yaltırak C.; 2003: *Reply: "Characteristic features of the North Anatolian Fault in the eastern Marmara Region and its tectonic evolution"*. Marine Geology, **194**, 203-208.

Ambraseys N.; 2001: *The earthquake of 10 July 1894 in the Gulf of İzmit (Turkey) and its relation to the earthquake of 17 August 1999*. J. of Seismology, **5**, 117-128.

Ambraseys N.; 2002a: *Seismic sea-waves in the Marmara Sea region during the last 20 centuries*. J. of Seismology, **6**, 571-578.

Ambraseys N.; 2002b: *The seismic activity of the Marmara Sea region over the last 2000 Years*. Bull. Seism. Soc. Am., **92**, 1, 1-18.

Ambraseys C.F. and Finkel B.; 1991: *Long term seismicity of the Istanbul and of the Marmara Sea region*. Terra Nova, **3**, 527-539.

Aochi H. and Madariaga R.; 2003: *The 1999 İzmit, Turkey, Earthquake: Nonplanar Fault Structure, Dynamic Rupture Process, and Strong Ground Motion*. Bull. Seism. Soc. Am., **93**, 1249-1266.

Armijo R., Meyer B., Hubert A., Barka A., de Chabalier J.B., Hubert-Ferrari A. and Çakır Z.; 2000: *The fault breaks of the 1999 earthquakes in Turkey and the tectonic evolution of the Sea of Marmara: a summary.* In: Barka A., Kozacı Ö., Akyüz S. and Altunel E. (eds), The 1999 İzmit and Düzce earthquakes: preliminary results, ITU Press, Istanbul, pp. 55–62.

Armijo R., Meyer B., Navarro S., King G. and Barka A.; 2002: *Asimmetric slip partitioning in the Sea of Marmara pull-apart: a clue to propagation processes of the North Anatolian Fault?* Terra Nova, **14**, 80-86.

Armijo R., Pondard N., Meyer B., Mercier de Lepinay B., Ucarkus G., Malavieille J., Dominguez S., Gustcher M.-A. Beck, Çagatay N., Cakir Z., Imren C., Kadir E. and MARMARASCARPS cruise party; 2005: *Submarine fault scarps in the Sea of Marmara pull-apart (North Anatolian Fault): implications for seismic hazard in Istanbul*. Geochem., Geophys., Geosyst., **6**, 1-29.

Awata Y., Yoshioka T., Emre Ö., Duman T.Y., Doğan A., Tsukuda E., Okamura M., Matsuoka H. and Kuşçu İ.; 2003: *Outline of the surface rupture of 1999 İzmit earthquake*. In: Emre Ö., Awata Y., Duman T.Y. (eds), Surface rupture associated with the 17 August 1999 İzmit Earthquake. Ankara, General Directorate of Mineral Research and Exploration Spec. Publ. 1, 41–55.

Barka A.A.; 1997: *Neotectonics of the Marmara region in active tectonics of Northwest Anatolia*. In: Schindler C. and Pfister M. (eds), The Marmara Poly-project. Hochschulverlag AG, ETH, Zurich.

Barka A.A., Kadinsky-Cade K.; 1988: *Strike-slip fault geometry in Turkey and its influence on earthquake activity*. Tectonics, **7**, 663-684.

Barka, A.A. and Kuşçu, I.; 1996: *Extends of the North Anatolian Fault in the İzmit, Gemlik and Bandirma Bays*. Turkish J. of Mar. Sci., **2**, 93-106.

Barka A.A., Kozaci Ö., Akyüz S. and Altunel E. (eds); 2000: *1999 İzmit and Düzce earthquakes: preliminary results*, Istanbul Technical University, ISBN 975-561-182-7.

Barka A.A., Akyüz H.S., Altunel E., Sunal G., Çakır Z., Dikbas A., Yerli B., Armijo R., Meyer B., de Chabalier J.B., Rockwell T., Dolan J.R., Hartleb R., Dawson T., Christofferson S., Tucker A., Fumal T., Langridge R., Stenner H., Lettis W., Bachhuber J. and Page W.; 2002: *The Surface Rupture and Slip Distribution of the 17 August 1999 İzmit Earthquake (M 7.4)*. North Anatolian Fault, Bull. Seism. Soc. Am., **92**, 43-60.

Bertrand S., Doner L., Akçer Ön S., Sancar U., Schudack U., Mischke M.N., Çağatay N. and Leroy S.A.G.; 2011: *Sedimentary record of coseismic subsidence in Hersek coastal lagoon (İzmit Bay, Turkey) and the late Holocene activity of the North Anatolian Fault*. Geochem., Geophys. Geosyst., **12**, Q06002.

Bohnhoff M., Grosser H. and Dresen G.; 2006: *Strain partitioning and stress rotation at the North Anatolian fault zone from aftershock focal mechanisms of the 1999 İzmit Mw = 7.4 earthquake*. Geophys. J. Int., **166**, 373-385.

Bouchon M., Toksöz M.N., Karabulut H., Bouin M.P., Dietrich M., Aktar M. and Edie M.; 2002: *Space and time evolution of rupture and faulting during the 1999 İzmit (Turkey) earthquake*. Bull. Seism. Soc. Am., **92**, 256-266.

Bozkurt E.; 2001: *Neotectonics of Turkey – a synthesis*. Geodinamica Acta, **14**, 3-30.

Çakır Z., de Chabalier J.-B., Armijo R., Meyer B., Barka A. and Peltzer G.; 2003: *Coseismic and early post-seismic slip associated with the 1999 İzmit earthquake (Turkey), from SAR interferometry and tectonic field observations*. Geophys. J. Int., **155**, 93–110.

Çağatay N., Görür N., Polonia A., Demirbağ E., Sakınç M., Cormier M.H., Capotondi L., McHugh C., Emre Ö. and Eris K.; 2003: *Sea-level changes and depositional environments in the İzmit Gulf, eastern Marmara Sea, during the late glacial Holocene period*. Marine Geology, **202**, 159-173.

Çağatay N., Görür N., Flecker R., Sakınç M.,Tünoğlu C., Ellam R., Krijgsman W., Vincent S., Dikbaş A.; 2006: *Paratethyan–Mediterranean connectivity in the Sea of Marmara region (NW Turkey) during the Messinian*. Sedimentary Geology, **188–189**, 171–187.

Carton H., Singh S.C., Hirn A., Bazin S., de Voogd B., Vigner A., Ricolleau A., Cetin S., Ocakoglu N., Karakoc F. and Sevilgen V.; 2007: *Seismic imaging of the three-dimensional architecture of the Çınarcık Basin along the North Anatolian Fault*. J. of Geophysical Research, **112**, 1-17.

Çetin O., Çetin T. and Ukav I.; 1995: *ESR dating of fossil mollusk shells observed in Quaternary Sequence in the Gulf of İzmit "Hersek Burnu-Kaba Burun"*. In: Meriç E. (ed), Quaternary sequence in the Gulf of İzmit, Turkish Navy Press, Istanbul, pp. 269–275 (in Turkish).

Cormier M.H., Seeber L., McHugh C.M.G., Polonia A., Çağatay N., Emre Ö., Gasperini L., Görür N., Bortoluzzi G., Bonatti E., Ryan W.B.F. and Newman K.R.; 2006: *North Anatolian Fault in the Gulf of İzmit (Turkey): rapid vertical motion in response to minor bends of a nonvertical continental transform*. J. of Geophysical Research, **111**, 1-25.

Crampin, S. and Evans R.; 1986: *Neotectonics of the Marmara Sea region of Turkey*. J. Geol. Soc. London, **143**, 343-346.

Demirbağ E., Rangin C., Le Pichon X. and Şengör A.M.C.; 2003: *Investigation of the tectonics of the Main Marmara Fault by means of deep-towed seismic data*. Tectonophysics, **361**, 1-19.

Dolu E., Gökaşan E., Meriç E., Ergin M., Görüm T., Tur H., Ecevitoğlu B., Avşar N., Görmüş M., Batuk F., Tok B. and Çetin O.; 2007: *Quaternary evolution of the Gulf of İzmit (NW Turkey): a sedimentary basin under control of the North Anatolian Fault Zone*. Geo-Marine Letters of International J. of Marine Geology, **27**, 355-381.

Ediger V. and Ergin M.; 1995: *Sedimentology of the Quaternary sequence in the Gulf of İzmit "Hersek Burnu-Kaba Burnu"*. In: Meriç E. (ed), Quaternary sequence in the Gulf of İzmit, Turkish Navy Press, Istanbul, pp. 241-250 (in Turkish).

Emre Ö. and Awata Y.; 2003: *Neotectonic characteristics of the North Anatolian Fault System in the eastern Marmara region*. In: Emre Ö., Awata Y. and Duman T.Y. (eds), Surface rupture associated with the 17 August 1999 İzmit Earthquake. Ankara, General Directorate of Mineral Research and Exploration Spec. Publ., 1, pp. 31–39.

Emre Ö., Erkal T., Tchepalyga A., Kazanci N., Keçer M. and Ünay E.; 1998: *Neogene-Quaternary evolution of the Eastern Marmara Region, Northwest Turkey*. Bull. Miner. Res. Explor. Inst. Turk., **120**, 119-145.

Ferrante V.; 2005: *Structural aspect and neotectonic of the North Anatolian Fault in the İzmit Gulf – Marmara Sea, Turkey*. Unpublished PhD thesis, University of Rome "La Sapienza" (in Italian).

Flerit F., Armijo R., King G.C.P., Meyer B. and Barka A.; 2003: *Slip partitioning in the Sea of Marmara pull-apart determined from GPS velocity vectors*. Geophys. J. Int., **154**, 1-7.

Forte E., Sugan M., Pipan M., Del Ben A. and Gasperini L.; 2009: Recent evolution and seismogenetic structures of Hersek Peninsula (Turkey) from high resolution seismic reflection data. In: 71st EAGE Conference & Exhibition, Amsterdam, The Netherlands, 8-11 June 2009, pp. 431-435.

Gasperini L., Polonia A., Bortoluzzi G., Henry P., Le Pichon X., Tryon M., Çağatay M.N. and Géli L.; 2011: *How far did the surface rupture of the 1999 İzmit earthquake reach in the Sea of Marmara?* Tectonics, **30**, TC1010, 1-11.

Garotta R.; 1999: *Shear waves from acquisition to interpretation*. 2000 DISC, SEG, Tulsa, OK, USA, ISBN 1-56080-093-3.

Gökaşan E., Alpar B., Gazioglu C., Yucel Z.Y., Tok B., Dogan E. and Güneysu C.; 2001: *Active tectonics of the İzmit Gulf (NE Marmara Sea): from high resolution seismic and multi-beam bathymetry data*. Marine Geology, **175**, 273-296.

Gökaşan E., Ustaömer T., Gazioglu C., Yucel Z.Y., Öztürk K., Tur H., Ecevitoglu B. and Tok B; 2003: *Morpho-tectonic evolution of the Marmara Sea inferred from multi-beam bathymetric and seismic data*. Geo-Marine Letters, **23**(1), 19-33.

Görür N., Çagatay M.N., Sakınç M., Sümengen M., Sentürk K., Yaltırak C. and Tchapalyga A.; 1997: *Origin of the Sea of Marmara as deduced from Neogene to Quaternary paleogeographic evolution of its frame*. Int. Geol. Rev., **39**, 342-352.

Gülen L., Pinar A., Kalafat D., Özel N., Horasan G., Yilmazer M. and Işikara A.M.; 2002: *Surface Fault Breaks, Aftershock Distribution, and Rupture Process of the 17 August 1999 İzmit, Turkey Earthquake*. Bull. Seism. Soc. Am., **92**, 230-244.

İmren C., Le Pichon X., Rangin C., Demirbağ E., Ecevitoglu B. and Görür N.; 2001: *The North Anatolian Fault within the Sea of Marmara: a new interpretation based on multi-channel seismic and multibeam bathymetry data*. Earth and Planetary Sc. Letters, **186**, 143-158.

Karabulut H., Bouin M.-P., Bouchon M., Dietrich M., Cornou C. and Aktar M.; 2002: *The seismicity in the Eastern Marmara Sea after the 17 August 1999 İzmit earthquake*. Bull. Seism. Soc. Am., **92**, 387–393.

Kozaci Ö, Altunel E., Lindvall S., Brankman C. and Lettis W.; 2011: *The North Anatolian Fault on Hersek Peninsula, Turkey: Its Geometry and Implications on 1999 İzmit Earthquake Rupture Propagation*. Turkish J. of Earth Sciences, **20**, 359-378.

Kurt H. and Yücesoy E.; 2009: *Submarine Structures in the Gulf of İzmit, based on Multichannel Seismic Reflection and Multibeam Bathymetry*. Marine Geophysical Researches, **30**, 73-**84.**

Kurt H., Sorlien C.C., Seeber L., Steckler M.S., Shillington D.J., Cifci G., Cormier M.-H., Dessa J.-X., Atgin O., Dondurur D., Demirbag E., Okay S., İmren C., Gurcay S. and Carton H.; 2013: *Steady late Quaternary slip rate on the Cinarcik section of the North Anatolian fault near Istanbul, Turkey*. Geophysical Research Letters, **40**, 4555-4559.

Kuşçu I., Okamura M., Matsuoka H. and Awata Y.; 2002: *Active faults in the Gulf of İzmit on the North Anatolian Fault, NW Turkey: a high-resolution shallow seismic study*. Marine Geology, **190**, 421-443.

Le Pichon X., Taymaz T. and Şengör A.M.C.; 1999: The *Marmara Fault and the future Istanbul earthquake*. In: Proceedings of the International Conference on the Kocaeli Earthquake, 17 August 1999, pp. 41-54.

Le Pichon X., Şengör A.M.C., Demirbağ E., Rangin C., Imren C., Armijo R., Görür N., Çağatay N., de Lepinay B.M., Meyer B., Saatçilar R. and Tok B.; 2001: *The active main Marmara fault*. Earth and Planetary Sc. Letters, **192**, 595-616.

Lettis W., Bachhuber J., Barka A., Witter R. and Brankman C.; 2000: *Surface fault rupture and segmentation during the Kocaeli earthquake*. In: Barka A., Kozacı Ö., Akyüz S. and Altunel E. (eds), The 1999 İzmit and Düzce earthquakes: preliminary results, ITU Press, Istanbul, pp. 31–54.

Lettis W., Bachhuber J., Witter R., Brankman C., Randolph C.E., Barka A., Page W.D. and Kaya A.; 2002: *Influence of releasing step over on surface fault rupture and fault segmentation: examples from the 17 August 1999 İzmit earthquake on the North Anatolian Fault, Turkey*. Bull. Seism. Soc. Am., **92**, 19-42.

Lin J. and Stein R.S.; 2004: *Stress triggering in thrust and subduction earthquakes and stress interaction between the southern San Andreas and nearby thrust and strike-slip faults*. J. Geophys. Res., **109**, B02303.

Meriç E., Yanko V. and Avşar N.; 1995: *Foraminiferal fauna of the Quaternary sequence in the Gulf of İzmit "Hersek Burnu-Kaba Burun"*. In: Meriç E. (ed), Quaternary sequence in the Gulf of İzmit, Turkish Navy Press, Istanbul, pp. 105–151 (in Turkish).

Okay A.I., Kaslilar-Ozcan A., Imren C., Boztepe-Guney A., Demirbağ E. and Kuşçu I.; 2000: *Active faults and evolving strike-slip basins in the Marmara Sea, northwest Turkey: a multichannel seismic reflection study*. Tectonophysics, **321**, 189-218.

Okyar M., Pınar A., Tezcan D. and Kamacı Z.; 2008: *Late quaternary seismic stratigraphy and active faults of the Gulf of İzmit (NE Marmara Sea)*. Marine Geophysical Research, **29**, 89-107.

Özaksoy V., Emre Ö., Yildirim C., Doğan A., Özalp S and Tokay F.; 2010: *Sedimentary record of late Holocene seismicity and uplift of Hersek restraining bend along the North Anatolian Fault in the Gulf of İzmit*. Tectonophysics, **487**, 33-45.

Özalaybey S., Ergin M., Aktar M., Tapırdamaz C., Biçmen F. and Yörük A.; 2002: *The 1999 İzmit earthquake sequence in Turkey: seismological and tectonic aspects*. Bull. Seism. Soc. Am., **92**, 376-386.

Paluska A., Poetsch S. and Bagrgu S.; 1989: *Tectonics, paleoseismic activity and recent deformation mechanism in the Sapanca-abant region (NW Turkey, North Anatolian Fault Zone)*. In: Turkish-German Earthquake Research Project. Earth Research Institute, Ankara, Turkey, Univ. of Kiel, West Germany, pp. 18-33.

Parke J.R., Minshull T.A., Anderson G., White R.S., McKenzie D., Kuşçu I., Bull J.M., Görür, N. and Şengör C.; 1999: *Active faults in the Sea of Marmara, western Turkey, imaged by seismic reflection profiles*. Terra Nova, **11**, 223-227.

Polat O., Haessler H., Cisternas A., Philip H., Eyidogan H., Aktar M., Frogneux M., Comte D. and Gürbüz C.; 2002: *The İzmit (Kocaeli), Turkey Earthquake of 17 August 1999: Previous Seismicity, Aftershocks, and Seismotectonics*. Bull. Seism. Soc. Am., **92**, 361-375.

Polonia A., Cormier M.H., Çağatay M.N, Bortoluzzi G., Bonatti E., Gasperini L., Ligi M., Capotondi L., Seeber L., McHugh C.M.G., Ryan W.B.F., Görür N., Emre Ö., Tok B., and the MARMARA2000 and MARMARA2001 scientific parties; 2002: *Exploring submarine earthquake geology in the Marmara Sea*. EOS Trans. Am. Geophys. U., **82**, 229 and 235-236.

Polonia A., Gasperini L., Amorosi A., Bonatti E., Bortoluzzi G., Çağatay N., Capotondi L., Cormier M.H., Görür N., McHigh C. and Seeber L.; 2004: *Holocene slip rate of the Northern Anatolian Fault beneath the Sea of Marmara*. Earth and Planet. Science Letters, **227**, 411-426.

Rangin C. and Le Pichon X.; 2004: *Strain localization in the Sea of Marmara: Propagation of the North Anatolian Fault in a now inactive pull-apart*. Tectonics, **23**, 1-17.

Reilinger R.E., Ergintav S., Burgmann R., McClusky S., Lenk O., Barka A., Gurkan O., Hearn L., Feigl K.L., Cakmak R., Aktug B., Ozener H. and Toksoz M.N.; 2000: *Coseismic and Postseismic Fault Slip for the 17 August 1999, M = 7.5, İzmit, Turkey Earthquake*. Science, **289**, Issue 5484, 1519-1524.

Sakınç M. and Bargu S.; 1989: *Stratigraphy of late Pleistocene (Tyrrenian) sediments in the south of the Gulf of İzmit and neotectonic characteristics of the region*. Geological Bulletin of Turkey, **32**, 51-64 (in Turkish).

Saroglu F., Emre Ö. and Boray A.; 1987: *Active faults of Turkey*. General Directorate of Mineral Research and Exploration (MTA), Report No. 8643, Ankara, 394 pp.

Şengör A.M.C.; 1979: *The North Anatolian transform fault: its age, offset and tectonic significance*. J. Geol. Soc. London, **136**, 269-282.

Şengör A.M.C., Görür N. and Saroglu F.; 1985: *Strike-slip faulting and related basin formation in zones of tectonic escape: Turkey as a case study*. In: Biddle K.D. and Christie-Blick N. (eds) Strike-slip deformation, basin formation, and sedimentation, SEPM Spec. Publ.17, pp. 227-264.

Şengör A.M.C., Tuysuz O., Imren C., Sakınç M., Eyidogan H., Görür N., Le Pichon X. and Claude Rangin C.; 2004: *The North Anatolian Fault. A new look*. Ann. Rev. Earth Planet. Sc., **33**, 1-75.

Toda S., Stein R.S., Richards-Dinger K. and Bozkurt S.B.; 2005: *Forecasting the evolution of seismicity in southern California: Animations built on earthquake stress transfer*. J. Geophys. Res., **110**, B05S16.

Uçarkuş G., Çakir Z. and Armijo R.; 2011: *Western termination of the Mw 7.4, 1999 İzmit earthquake rupture: implications for the expected large earthquake in the Sea of Marmara*. Turkish J. of Earth Sci., **20**, 379-394.

Witter C.R., Lettis W.R., Bachhuber J., Barka A., Evren E., Cakir Z., Page D.W., Hengesh J. and Seitz G.; 2000: *Paleoseismic trenching study across the Yalova segment of the North Anatolian Fault, Hersek Peninsula, Turkey*. In: Barka A., Kozacı Ö., Akyüz S. and Altunel E. (eds), The 1999 İzmit and Düzce earthquakes: preliminary results, ITU Press, Istanbul, pp. 329-339.

Wright T.J., Fielding E.J. and Parsons B.; 2001: *Triggered slip: observations of the 17 August 1999 İzmit (Turkey) earthquake using radar interferometry*. Geophys. Res. Lett., **28**, 1079-1082.

Yaltırak C.; 2002: *Tectonic evolution of the Marmara Sea and its surroundings*. Marine Geology, **190**, 494-529.

Corresponding author: Emanuele Forte
Dep. of Mathematics and Geosciences, University of Trieste
Via Weiss 1, 34128, Trieste, Italy
Phone: +39 0405582271; fax: +39 040 5582290; e-mail: eforte@units.it